https://doi.org/10.1093/plphys/kiad550 PLANT PHYSIOLOGY 2024: 194: 1006–1023

Plant Physiology®

Research Article

Citronellol biosynthesis in pelargonium is a multistep pathway involving progesterone 5β-reductase and/or iridoid synthase-like enzymes

Laure Martinelli,[1,2,†] **Camille Bihanic**,[1,†] **Aurélie Bony**,[1] **Florence Gros**,[1] **Corentin Conart**,[1] **Sébastien Fiorucci**,[3] **Hervé Casabianca**,[4] **Frédéric Schiets**,[4] **Giorgiana Chietera**,[5] **Benoît Boachon**,[1] **Bernard Blerot**,[5] **Sylvie Baudino**,[1] **Frédéric Jullien**[1,*] **and Denis Saint-Marcoux**[1]

1 Laboratoire BVpam—UMR 5079, Université Jean Monnet Saint-Étienne, CNRS, Saint-Étienne 42023, France
2 Department of Biochemistry, Max Planck Institute for Chemical Ecology, Jena 07455, Germany
3 Institut de Chimie de Nice—UMR 7272, Université Côte d'Azur, CNRS, Nice 06108, France
4 Institut des Sciences Analytiques—UMR 5280, Université de Lyon, CNRS, Villeurbanne 69100, France
5 IFF-LMR Naturals, Grasse 06130, France

*Author for correspondence: jullien@univ-st-etienne.fr
†These authors contributed equally.
The author responsible for distribution of materials integral to the findings presented in this article in accordance with the policy described in the Instructions for Authors (https://academic.oup.com/plphys/pages/General-Instructions) is Frédéric Jullien.

Abstract

Citronellol is a pleasant-smelling compound produced in rose (*Rosa* spp.) flowers and in the leaves of many aromatic plants, including pelargoniums (*Pelargonium* spp.). Although geraniol production has been well studied in several plants, citronellol biosynthesis has been documented only in crab-lipped spider orchid (*Caladenia plicata*) and its mechanism remains open to question in other species. We therefore profiled 10 pelargonium accessions using RNA sequencing and gas chromatography-MS analysis. Three enzymes from the progesterone 5β-reductase and/or iridoid synthase-like enzymes (PRISE) family were characterized in vitroand subsequently identified as citral reductases (named PhCIRs). Transgenic RNAi lines supported a role for PhCIRs in the biosynthesis of citronellol as well as in the production of mint-scented terpenes. Despite their high amino acid sequence identity, the 3 enzymes showed contrasting stereoselectivity, either producing mainly (*S*)-citronellal or a racemate of both (*R*)- and (*S*)-citronellal. Using site-directed mutagenesis, we identified a single amino acid substitution as being primarily responsible for the enzyme's enantioselectivity. Phylogenetic analysis of pelargonium PRISEs revealed 3 clades and 7 groups of orthologs. PRISEs from different groups exhibited differential affinities toward substrates (citral and progesterone) and cofactors (NADH/NADPH), but most were able to reduce both substrates, prompting hypotheses regarding the evolutionary history of PhCIRs. Our results demonstrate that pelargoniums evolved citronellol biosynthesis independently through a 3-step pathway involving PRISE homologs and both citral and citronellal as intermediates. In addition, these enzymes control the enantiomeric ratio of citronellol thanks to small alterations of the catalytic site.

Introduction

β-citronellol (hereafter referred to as citronellol) is a volatile organic compound, more accurately a monoterpene alcohol with an intense roselike scent. It is commonly produced by the flowers of orchids and roses, as well as by the vegetative organs of several plants like lemongrass (*Cymbopogon* spp.), lemon-scented gum (*Corymbia citriodora*), ginger (*Zingiber officinale*), and pelargonium (*Pelargonium* spp.). Due to the

Received June 21, 2023. Accepted September 25, 2023. Advance access publication October 13, 2023

absence of the C=C double bond in C2–C3, which is present in geraniol, citronellol has 2 enantiomeric forms. In rose (*Rosa* sp.), grape (*Vitis vinifera*), pelargonium, and the crab-lipped spider orchid (*Caladenia plicata*), (*S*)-citronellol is the major enantiomer (Ravid et al. 1992; Luan et al. 2005; Xu et al. 2017), whereas (*R*)-citronellol dominates in *Boronia citriodora* and citronella (*Cymbopogon nardus*) (Duretto 2003; Surburg and Panten 2006). Few ecological roles have been documented for citronellol. Still, (*S*)-citronellol has been demonstrated to act as a pollinator attractant in *C. plicata* (Xu et al. 2017), while recently, an arthropod chemosensory receptor was characterized, strengthening the role of citronellol as a natural repellent and, more broadly, in plant defense mechanisms (Tian et al. 2022).

Multiple studies in rose (Dunphy and Allcock 1972), grape (Luan et al. 2005), ginger (Iijima et al. 2014), and *C. plicata* (Xu et al. 2017) clearly demonstrated that citronellol is derived from geraniol. In the latter, citronellol was biosynthesized via a 3-step pathway, with the geranial reductase CpGER1 (Xu et al. 2017) reducing citral, a mix of the tautomers geranial ((*E*)-citral) and neral ((*Z*)-citral), to citronellal and an alcohol dehydrogenase (ADH) completing the pathway by catalyzing the conversion of geraniol to citral and citronellal to citronellol (Fig. 1). CpGER1 belongs to the progesterone 5β-reductase and/or iridoid synthase-like enzymes (PRISE) family (Petersen et al. 2016), part of the short-chain dehydrogenase reductase (SDR) superfamily. The PRISE family groups progesterone 5β-reductases (P5βR), which stereospecifically reduce progesterone to 5β-pregnane-3,20-dione, leading to cardenolide biosynthesis (Gärtner et al. 1994; Herl et al. 2006; Munkert et al. 2011), and iridoid synthases (ISY), which catalyze the reduction and cyclization of 8-oxogeranial, leading to iridoid biosynthesis (Geu-Flores et al. 2012; Xiang et al. 2017). Aside from progesterone, 8-oxogeranial, and citral, PRISEs also accept several 1,4-enones, such as 2-cyclohexen-1-one or methyl vinyl ketone, and are known for having a wide spectrum of substrates.

Contrasting with the 3-step pathway discovered in *C. plicata*, labeling and feeding experiments indicate a possible direct reduction of geraniol to citronellol in other species (Dunphy and Allcock 1972; Suga and Shishibori 1973; Banthorpe et al. 1983; Luan et al. 2005). Moreover, ginger rhizome fed with deuterated geraniol led to 2 different labeling patterns in citronellol, raising the possibility of the coexistence of both a direct and a multistep biosynthetic pathway in this species (Iijima et al. 2014). Enzymes from the 12-oxophytodienoate reductase (OPR) family were considered to be good candidates for a direct reduction of geraniol to citronellol (Fig. 1) based on the ability of the *Hevea brasiliensis* homologs to perform this reaction in vitro (Yuan et al. 2011). On the other hand, several OPRs isolated from a rose-scented pelargonium were unable to reduce geraniol. However, these enzymes could reduce citral to citronellal (Iijima et al. 2016), but their physiological role as citral reductases remains untested.

The genus *Pelargonium* consists of almost 280 species and includes scented species and hybrids. Of these, the pelargonium rosat hybrids, often referred to as *Pelargonium* × *hybridum* cv. rosat (*P.* rosat) and occasionally as *Pelargonium graveolens* hybrids, are particularly famous for their rose-scented essential oil (EO), which is widely used by fragrance and cosmetic industries (Demarne 2002; Verma et al. 2016). *Pelargonium* rosat resulted from crosses between 1 rose-scented parent, *Pelargonium capitatum*, and 1 mint-scented parent, presumably *Pelargonium radens* or *P. graveolens*. Pelargonium EO is mainly composed of monoterpenes, and the 4 main hybrids—named *P.* rosat 'Bourbon', 'China', 'Egypt' and 'Grasse', according to their production areas—are rich in geraniol, citronellol, their aldehydes counterparts, and various ester derivatives (Gauvin et al. 2004; Juliani et al. 2006). Fragrance industries pay special attention to the geraniol/citronellol ratio of pelargonium EO, as it affects the final odor profile and quality (Doimo et al. 1999; Verma et al. 2013). Consequently, pelargonium makes an ideal plant model to better understand the steps required for citronellol biosynthesis. A geraniol synthase (PhGES) responsible for the biosynthesis of geraniol from geranyl diphosphate (GPP) was characterized in several *P.* rosats (Blerot et al. 2018), but how geraniol is reduced to citronellol, including whether directly or indirectly, remains unknown. Recently, a possible route (Fig. 1) suggested a reduction of geranyl phosphate (GP) to citronellyl phosphate (CP), followed by a dephosphorylation of CP to citronellol (Bergman et al. 2021). In this case, a nucleotide diphosphates bound to X (NUDIX) hydrolase would ensure the conversion of GPP to GP, thus mimicking the biosynthesis of geraniol in rose (Magnard et al. 2015). In summary, the citronellol biosynthetic pathways in pelargonium are only partially characterized and are still under debate.

Here, we demonstrate that citronellol biosynthesis in pelargonium is a 3-step process starting from geraniol and involving 3 closely related enzymes belonging to the PRISE family. Dubbed PhCIR for *P.* × *hybridum* citral reductase, these 3 enzymes reduce citral to citronellal and present contrasted stereoselectivities. As such, 2 of the enzymes produce about 90% (*S*)-citronellal and 10% (*R*)-citronellal, whereas the third produces a racemic mixture. We took advantage of the quasi-identity between the enzyme sequences to investigate which amino acids were involved in their enantioselectivity and were able to show that a single amino acid of the active site is involved in the enantiomeric switch observed. Furthermore, our results indicate that PhCIRs likely have a role in the production of mint-scented compounds, thus placing these enzymes as central actors of the terpene production in pelargoniums. Finally, our study shows that PRISE members belonging to distant clades were recruited in parallel during evolution to ensure the citral reduction step of the citronellol biosynthetic pathway.

Results

Multiomic screening for reductase candidates

To unravel the biosynthetic pathway of citronellol in pelargoniums, we chose a multiomic approach associating gene expression with chemical phenotypes of several accessions. As

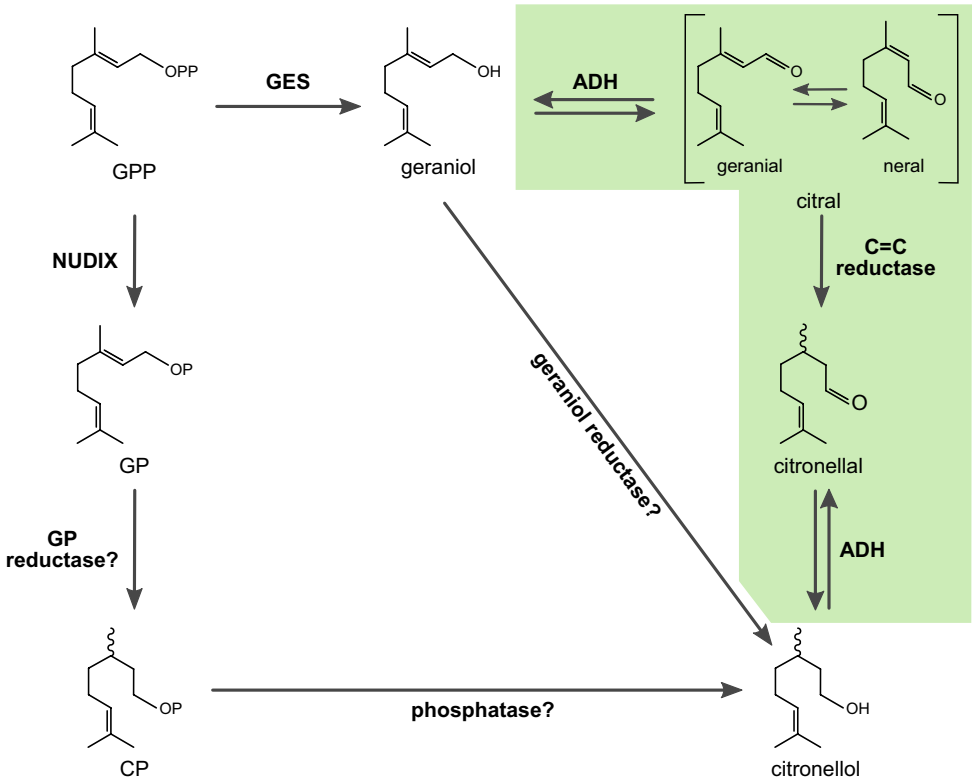

Figure 1. Three hypothetic routes for the biosynthesis of citronellol in pelargonium. Direct reduction of geraniol, synthesized by a geraniol synthase (GES), to citronellol was suggested by in vitro activity of OPRs from *H. brasiliensis* (Yuan et al. 2011). A 3-step pathway starting from geraniol (green box) has been demonstrated in *C. plicata* by Xu et al. (2017); it involves ADH and a citral reductase from the PRISE family. OPRs could fulfill the role of a C=C reductase according to the work of Iijima et al. (2016) in rose-scented pelargonium. Finally, in rose-scented pelargonium, Bergman et al. (2021) proposed the action of a NUDIX hydrolase to convert GPP to GP. GP is then reduced to CP, and a putative phosphatase would dephosphorylate CP to citronellol. Question marks indicate the lack of enzyme characterization for this proposed step.

such, young leaves of 10 scented accessions with known EO composition (Lis-Balchin 1991; Demarne and Van der Walt 1993; Lalli et al. 2006; Blerot et al. 2016) were sampled and divided in 2, so that terpenoid content and gene expression could be determined on the same sample.

All 10 accessions displayed clear differences in the content of geraniol, citronellol, their aldehyde counterparts, and their ester derivatives (Fig. 2). The 4 rosat hybrids, *P. capitatum* and *P.* × 'Toussaint', accumulated various amounts of geraniol and citronellol in different relative proportions. Both *P. radens* and *P. graveolens* showed a complete lack of geraniol, citronellol, or their aldehydes counterparts and ester derivatives. *P.* 'Prince of Orange' produced only geraniol and its esters in small quantities but accumulated neither citral, citronellal, nor citronellol. Finally, *Pelargonium citronellum* accumulated high levels of citral but no citronellal nor citronellol. The presence of accumulated citral and sometimes citronellal in all citronellol-producing accessions tended to indicate that the targeted reductase was involved in a pathway starting from geraniol and involving citral and citronellal as intermediates.

In the absence of any common reference such as a sequenced genome, transcriptomes of each accession were de novo assembled and 84 PRISEs and 46 OPR candidates were identified. To properly relate the expression of *PRISE* and *OPR* transcripts with the citronellol pathway compounds, orthologous and paralogous relationships needed to be determined across the different accessions by inferring a maximum-likelihood phylogenetic tree based on protein sequences for each family.

Pelargonium PRISE sequences clustered in 3 distinct clades (Fig. 3). Interestingly, clade I contained sequences from biochemically characterized enzymes, including citral reductases from *Plantago major* (PmMOR; *P. major* multisubstrate oxidoreductase) and *C. plicata* (CpGER1; *C. plicata* geraniol reductase 1) and 5 ISYs from Madagascar periwinkle (*Catharanthus roseus*) (Munkert et al. 2015). Clade II included mainly pelargonium sequences, as well as 2 sequences from the orchid *Apostasia shenzhenica* and 1 *C. roseus* enzyme (Munkert et al. 2015; Zhang et al. 2017). Finally, clade III was defined by pelargonium species and 1 *Arabidopsis thaliana* sequence.

Based on phylogenetic distances, statistical support, and accession representation, 7 PRISE putative groups of pelargonium orthologs were defined. Transcripts corresponding to the PRISE-4 group were strongly accumulated in young

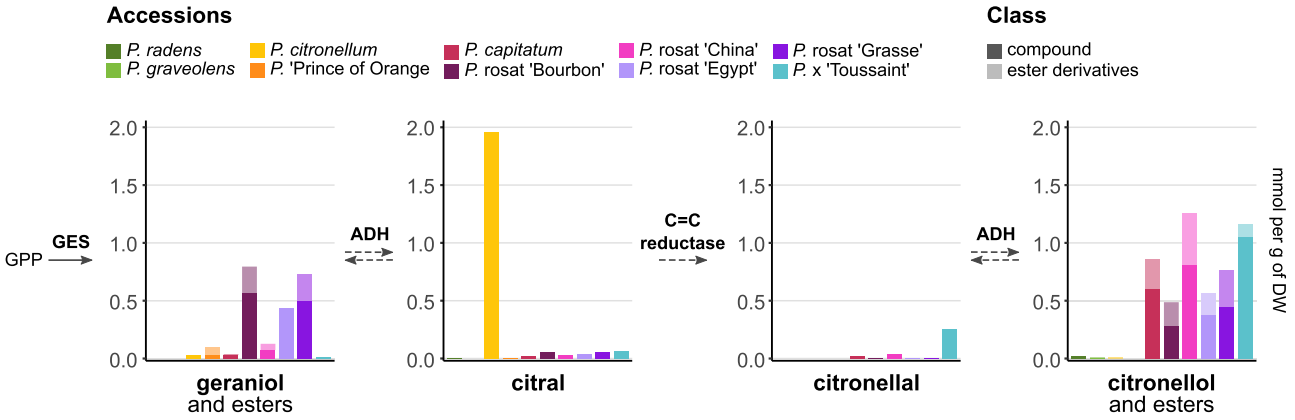

Figure 2. Accumulation of compounds involved in the citronellol pathway in 10 scented pelargoniums. Compounds were quantified by GC-MS analysis from hexane extracts (mmol per g of dry weight [DW]) of each accession. Barplots represent the mean ($n = 3$). The ester derivatives of geraniol and citronellol correspond to the sum of all detected respective esters. Citral corresponds to the sum of geranial and neral. ADH, alcohol dehydrogenase; GES, geraniol synthase; GPP, geranyl diphosphate.

leaves, with a maximum of ~70 zTPM for *pxhygr.c16865* in *P.* rosat 'Grasse' (Fig. 3). In contrast, transcripts from other groups were expressed about 10 to 100 times lower. The expression pattern of PRISE-4 transcripts was consistent with a role of the encoded enzymes in the reduction of citral to citronellal. As such, PRISE-4 transcripts were strongly expressed in the 4 rosat hybrids, *P. capitatum* and *P.* × 'Toussaint', all of which producing massive amounts of citronellol and citronellyls (Fig. 2). Accordingly, the PRISE-4 transcript in *P. citronellum*—an accession highly accumulating citral but no citronellal—was barely expressed. Interestingly, the 2 homologs of *P. radens* and *P. graveolens* were strongly expressed, even though these 2 accessions accumulated neither citronellal nor downstream compounds. Within the PRISE-4 group, several sequences of the same accession for which phylogenetic relationships were unclear showed a marked expression, notably in rosat hybrids.

Similarly to PRISEs, pelargonium OPR transcripts were clustered and 5 groups of orthology were defined (Supplemental Fig. S1). Strongly contrasting with PRISEs, OPRs transcript expression was low in all 5 groups (up to 3.5 zTPM). Importantly, none of them presented an expression pattern that could be related to the observed accumulation of geraniol, citral, citronellal, and citronellol in the 10 pelargonium accessions. Notably, *P. citronellum* transcripts were expressed in each group, with similar levels compared with homologs from accessions producing citronellol.

Taken together, these results indicated that PRISE homologs from the PRISE-4 group of orthology constituted the best reductase candidates for citronellol production. Given their weak expression level, OPR enzymes were excluded as candidate and not studied further.

Characterization of 3 citral reductases

Phylogenetic reconstruction of pelargonium PRISEs showed that PRISE-4 group contained multiple nearly identical assembled transcripts. To assess the reality of the 3 sequences inferred from *P.* rosat 'Grasse' short reads, long-read transcriptome sequencing was carried out on leaves sampled from identical developmental stage and 3 contigs corresponding to *pxhygr.c16865*, *pxhygr.t246355*, and *pxhygr.t251567* were identified (Supplemental Fig. S2A). Mapping the long reads or the short reads to the long-read transcriptome confirmed the ratio of expression observed between the transcripts (Supplemental Fig. S2B). PCR primers were designed so that the 3 transcripts could be amplified from leaf RNA of *P.* rosat 'Grasse' and 'Bourbon'. Several clones with some degree of polymorphism were obtained, corresponding to *pxhygr.c16865* and *pxhybo.t54784*—the transcript orthologous to *pxhygr.t246355* in *P.* rosat 'Bourbon'. Two sequences corresponding to *pxhygr.c16865* and one to *pxhybo.t54784* were further studied. The 3 shared a high degree of identity at the amino acid level (96%) and displayed all the typical PRISE motifs (Fig. 4A). No PCR product could be obtained for the third assembled transcript, *pxhygr.t251567*.

The capacity of the encoded enzymes to reduce citral was tested in vitro by incubation of the purified recombinant proteins in the presence of either NADH or NADPH cofactor. As shown in Figure 4, B and C, the 3 enzymes had comparable activities, reducing about 40% to 55% of citral to citronellal, while the reduced cofactor had a minor influence. The 3 enzymes could not reduce geraniol to citronellol nor to any other intermediate of the putative pathway. Consequently, the 2 enzymes corresponding to the assembled transcript *pxhygr.c16865* were named PhCIR1a and PhCIR1b; the enzyme corresponding to *pxhybo.t54784* was named PhCIR2.

To assess the capacity of the enzymes to reduce citral in leaf physiological conditions, PhCIR1a was transiently expressed in *Nicotiana benthamiana* leaves. Transformed leaf discs produced high quantities of citronellol in the presence of citral in the incubation buffer (Supplemental Fig. S3A and Table S1), as well as geraniol and nerol, while no citronellal could be observed. In contrast, only traces of citronellol could be detected with control leaf discs—transformed only with

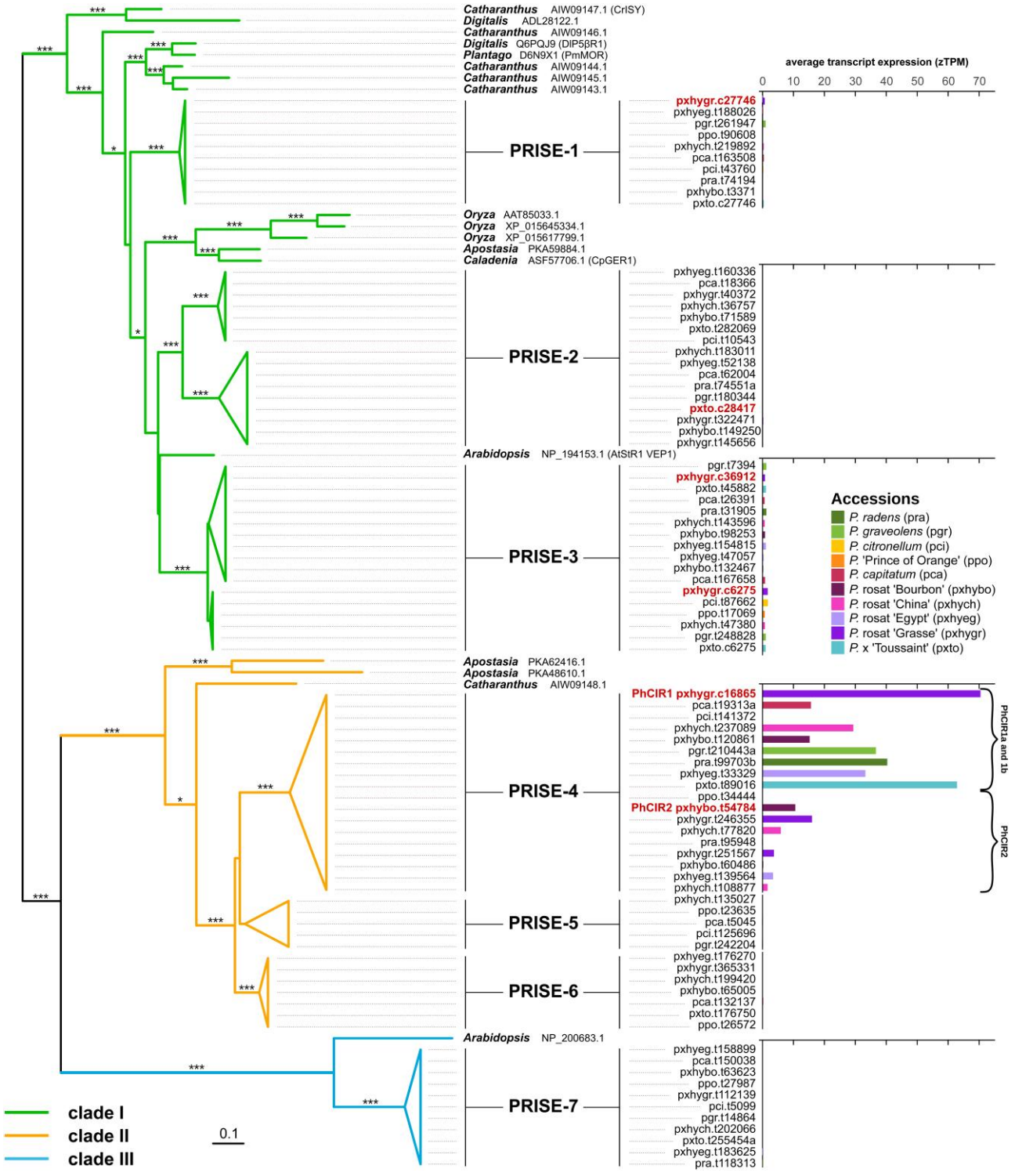

Figure 3. Expression of groups of pelargonium PRISE orthologous transcripts. *C. plicata* CpGER1 peptide sequence was used as query to retrieve sequences from the transcriptomes of the 10 pelargonium accessions, as well as from other databases (see Supplemental Data Set 2). A maximum-likelihood tree was inferred from the edited alignment using the JTTDCMUT + G model and ML optimization of amino acid substitution frequencies. Bootstrap values converged after 550 runs. Sequences from *A. thaliana*, *A. shenzhenica*, *C. plicata*, *C. roseus*, *D. lanata*, *P. major*, and *O. sativa* were included to help structuring the tree. Transcripts were manually clustered in 7 groups of putative orthologs (PRISE-1 to PRISE-7) based on phylogenetic distance and bootstrap support values of the clades and were collapsed with the help of FigTree v1.4.4 (github.com/rambaut/figtree). Proteins known to present a citral reducing activity had their name adjoined to the sequence identifier. Cloned sequences are indicated in red bold. Bootstrap support as follows: ***≥90%, **≥80%, and *≥70%. The tree scale bar represents the number of substitutions per site. Horizontal barplots represent the expression of each transcript as the standardized expression in transcripts per million (zTPM) averaged across the replicates ($n = 3$).

the P19 vector—likely resulting from endogenous reduction. The production of citronellol instead of citronellal by PhCIR1a-transformed leaf discs was likely the result of a fast reduction of the latter by ADHs endogenous to *N. benthamiana* leaves. Indeed, citronellal was almost completely reduced to citronellol both by control and PhCIR1a-transformed leaf discs (Supplemental Table S1). Similarly, endogenous ADHs were responsible for the diverse redox equilibrium observed between geraniol, citral, and nerol with control leaf discs, as well as the minute quantity of citronellol produced by transformed leaf discs incubated with geraniol (Supplemental Table S1). Transformed leaf discs could not oxidize citronellal to citral. These results indicated that PhCIR1a was able to act as a citral reductase in planta.

Finally, subcellular localization of PhCIR1a was assessed by transiently expressing the GFP-fused enzyme in *N. benthamiana* leaves. As shown in Supplemental Fig. S3B, PhCIR1a was localized in the cytosol, as expected from the in silico predictions.

Taken together, these results showed that pelargonium leaves expressed 3 different transcripts—of which 2 could not be distinguished in the transcriptome assembly—encoding 3 enzymes able to reduce citral to citronellal.

PhCIRs are expressed in glandular trichomes

In pelargonium, terpene biosynthesis and accumulation take place in glandular trichomes. Consequently, localization of *PhCIR* transcripts was investigated in the leaf. To this end, accumulation of *PhCIR* transcripts in *P. citronellum* and *P.* rosat 'Grasse' whole leaves or depleted of trichomes (Fig. 5A) was assessed. As expected, transcripts did not accumulate in *P. citronellum* (Fig. 5B), thus confirming the expression observed by transcriptomics (Fig. 3). In *P.* rosat 'Grasse', transcripts accumulated significantly less (3 times) in leaves depleted of trichomes, thus indicating that *PhCIRs* were expressed preferentially in glandular trichomes.

Shutting down *PhCIRs* expression impairs production of citronellol

To assess whether PhCIR enzymes were *in fine* involved in the biosynthesis of citronellol, RNAi mutants were generated by stable transformation of *P.* rosat 'Grasse' using *Agrobacterium rhizogenes*. The interference RNA was designed to target the sequences of the 3 PhCIRs but could not bind with PRISEs from other clades (Supplemental Fig. S4). Because *A. rhizogenes* is known to alter plant morphology, to increase EO production and to modify terpene composition (Pellegrineschi and Davolio-Mariani 1996), a transformation control was also produced using the WT bacteria strain. WT plants, WT *A. rhizogenes*–transformed plants and RNAi mutants were all morphologically identical. Eighteen RNAi plants were analyzed, of which only 3 displayed a chemical phenotype indistinguishable from the WT, whereas 13 displayed a drastic reduction of both *PhCIR* transcripts and citronellol accumulation (Fig. 6A). A finer analysis of 3 plants exhibiting a strong phenotype revealed that when *PhCIR* transcripts were accumulated to as little as 2% of the transformed control (Fig. 6B), citronellol and derivatives were reduced to <1% (Fig. 6, B to D); concomitantly, accumulation of geraniol, geranial, nerol, and neryl formate was increased and was approximately inversely proportional to the decrease of citronellol and citronellyl formate combined (Fig. 6, C and D). This suggests that in RNAi lines, excess citral resulting from the absence of any PhCIR activity is partially accumulated as geraniol and partially absorbed by an alternate pathway likely involving endogenous ADHs forming nerol. Moreover, this result supports the view that citronellol biosynthesis depends on sequential steps starting from geraniol. Thus, RNAi mutants clearly indicated that citronellol production in pelargonium is dependent upon the availability of the different PhCIR enzymes.

Surprisingly, RNAi plants lacking *PhCIRs* expression were devoid of isomenthone—a compound normally present in WT plants—and abnormally accumulated piperitone instead (Fig. 6, C and D). These results indicated that PhCIR enzymes might also play an important role in the *p*-menthane biosynthetic pathway that is yet to be determined.

Stereoselectivity of PhCIRs can be shifted by the substitution of a single amino acid of the catalytic site

Because citronellal contains an asymmetrical carbon, the stereoselectivity of the 3 PhCIRs was tested in vitro with NADH or NADPH as cofactors. PhCIR1a and PhCIR1b catalyzed mainly the synthesis of (*S*)-citronellal, respectively 92% and 97% in the presence of NADH (Fig. 7A). Strongly contrasting, PhCIR2 produced citronellal close to racemate (56% of (*S*)-citronellal).

To better understand which structural variation could determine this contrasted stereoselectivity, the crystal structure of a PRISE from *P. major* was used to model the 3 PhCIRs. The 3 proteins were folded into a Rossman-like domain—part of the active site cavity and responsible for the binding of the cofactor—and a C-terminal capping domain containing most of the substrate binding residues (Fig. 7B). Catalytic residues of the template aligned with K127 and Y160. These were conserved among the 3 PhCIRs and oriented toward the cofactor and the carbonyl functional group of the substrate, suggesting the same role in the enzymatic mechanism (Fig. 7C).

Despite being nearly identical, the 3 proteins presented a variable region from position 324 to 332 involving residues of the ligand-binding pocket: where PhCIR1a/b displayed a F(A/S)VNVEVQF motif, PhCIR2 sequence was YGLNLE VQW (Fig. 4A). Because the disparities of the 2 aromatic residues F324Y and F332W could explain the different stereoselectivities observed, 4 mutant proteins were generated by site-directed mutagenesis of PhCIR1b and PhCIR2, chosen for their close sequence proximity (Fig. 4A). The enantiomeric distribution of citronellal produced by the modified enzymes was determined in vitro (Fig. 7D). Substituting PhCIR1b F332 to a tryptophan had no effect, whereas

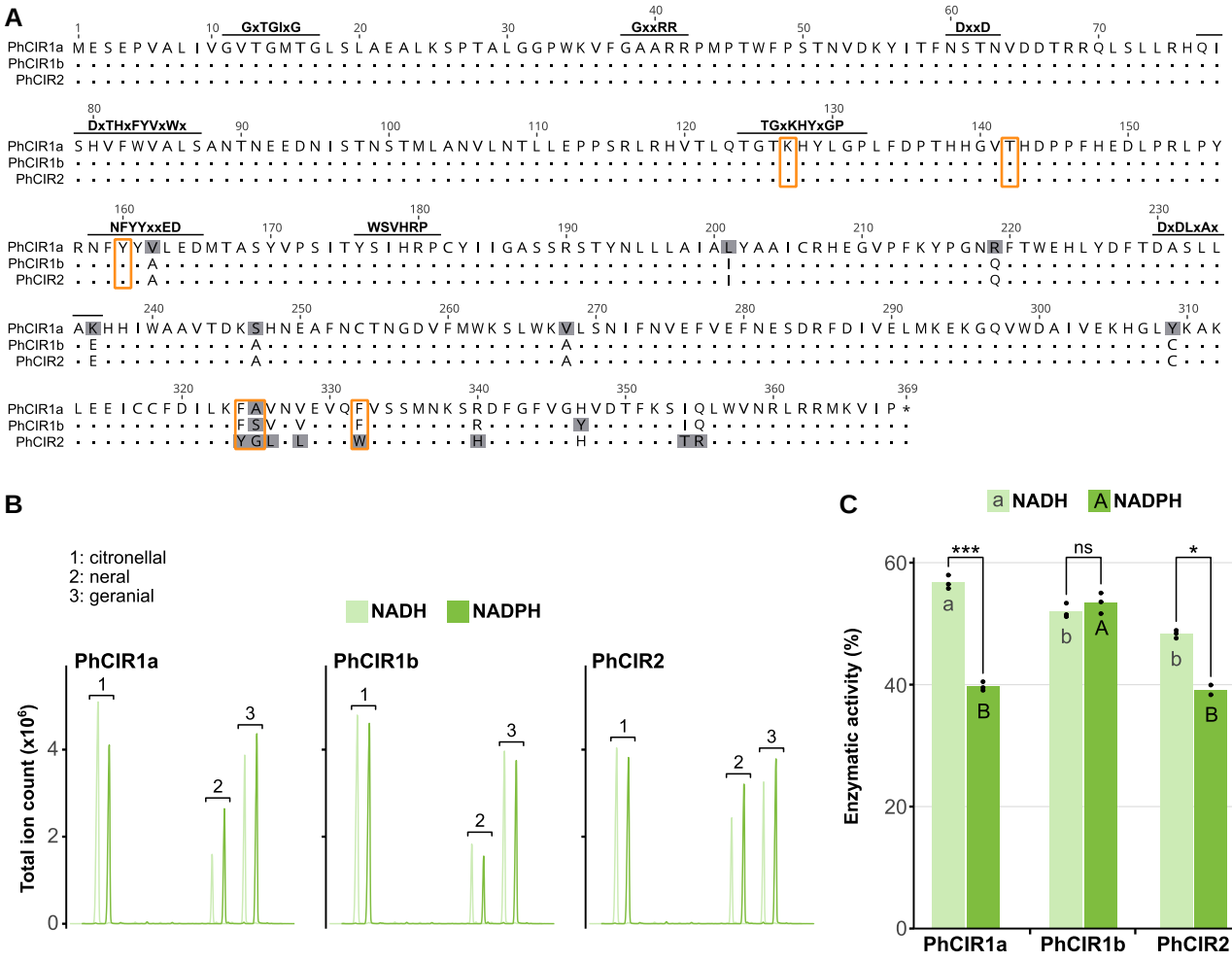

Figure 4. Biochemical characterization of 3 citral reductases. **A)** Protein sequence alignment of the 3 citral reductases from rose-scented pelargonium (PhCIRs) using the Geneious software. Amino acid differences between the 3 sequences (PhCIR1a, PhCIR1b, and PhCIR2) are highlighted in gray. Amino acids presumed to be involved in substrate binding (orange boxes) from the citral reducing PRISE (PmMOR) from *P. major* (Fellows et al. 2018) and sequence signature motifs of the PRISE family (black annotations) from Gavidia et al. (2007), Thorn et al. (2008), and Pérez-Bermúdez et al. (2010) are depicted. **B)** Chromatogram of in vitro enzymatic activities of the purified protein recombinant PhCIR1a, PhCIR1b, and PhCIR2, in the presence of citral and reduced cofactors (NADH or NADPH). **C)** Enzymatic activities presented in **B)** expressed as the percentage of citral reduced to citronellal. Barplots represent the mean ($n = 3$) and individual values are depicted with dots. Statistical differences between enzymes are outlined for each cofactor as letters per groups (ANOVA, followed by Tukey's test, $P < 0.01$), and the statistical difference according to the cofactor used is outlined for each enzyme (t test, ***$P < 0.01$, **$P < 0.01$, *$P < 0.05$, ns; $P > 0.05$). Chromatograms and compound accumulations were obtained by GC-MS analysis.

substituting PhCIR1b F324 to a tyrosine produced a significant, but marginal change. In contrast, the converse mutations performed on PhCIR2 had a stronger effect. Substituting PhCIR2 Y324 to a phenylalanine unbalanced the enantiomeric ratio, while substituting PhCIR2 W332 to a phenylalanine led to a major effect as the mutant PhCIR2^{W332F} catalyzed mainly the synthesis of (*S*)-citronellal, reaching 93% enantioselectivity, thus reminiscent of PhCIR1a/b phenotype.

Taken together, these results indicated that the ligand-binding pocket position 332 of PhCIRs can play a central role in determining the stereoselectivity of the enzymes, while the other aromatic residues had a lesser impact.

Pelargonium CIR enzymes evolved during early angiosperm history

The phylogenetic analysis of pelargonium PRISEs revealed several groups distributed into 3 clades (Fig. 3). Because PRISEs are known to be promiscuous enzymes with a large palette of substrates (Burda et al. 2009; Durchschein et al. 2012), the ability to reduce citral could be a common feature of pelargonium enzymes. To assess this possibility, representative sequences of the PRISE-1, -2, and -3 orthology groups (clade I) were cloned, and the corresponding enzymes were tested for their capacity to reduce citral and progesterone. All enzymes were able to reduce citral to citronellal (Supplemental Fig. S5A), with marked differences in terms

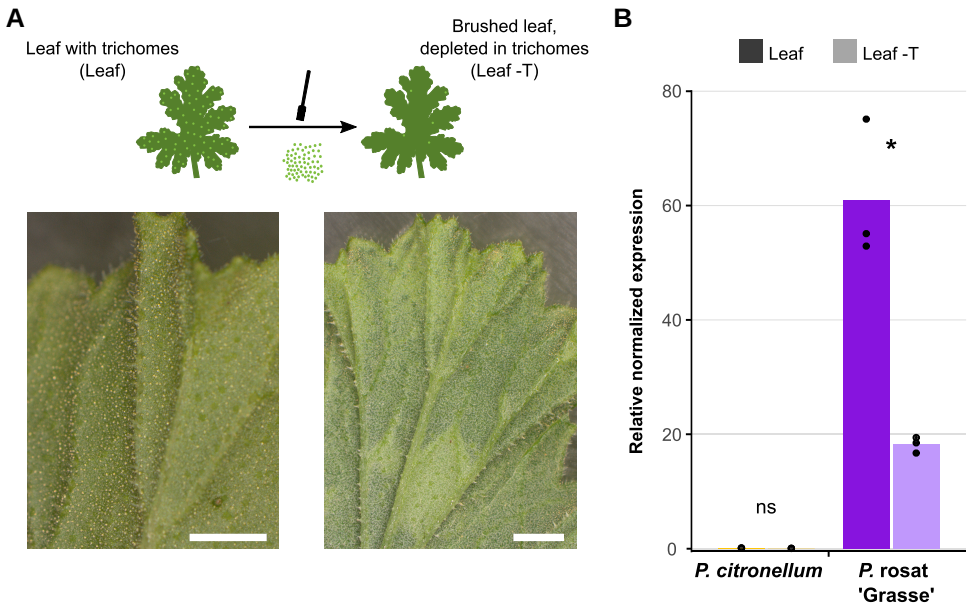

Figure 5. Transcript accumulation of PhCIRs in trichome-less leaves. Leaves were fast frozen in liquid nitrogen, and leaf surface was gently brushed with a cold brush to remove glandular trichomes. **A)** Photographs of whole and trichome-less pelargonium leaves. Scale bars correspond to 3 mm. **B)** Relative normalized expression of *PhCIRs* in whole and trichome-less leaves measured by RT-qPCR. Primers used probed the 3 transcripts equally (Supplemental Table S1). Transcript accumulation was normalized to the geometric mean expression of *β-ACTIN* and *α-TUBULIN*. Barplots represent the mean expression ($n = 3$) and individual values are depicted with dots. *t test, $P < 0.05$ significant difference.

of activity and affinity to the reduced cofactor, as compared with PhCIR1a (PRISE-4, clade II). For example, PRISE-2 representative entirely reduced citral in the presence of NADH but only 10% with NADPH. Comparatively, PhCIR1a presented a relative activity of 73% and 81%, respectively, to these cofactors. Previous studies linked variations in affinity for the 2 cofactors to conserved motifs (Thorn et al. 2008; Pérez-Bermúdez et al. 2010), in particular the GxxRR motif known to interact with the phosphate group of NADPH. However, all pelargonium PRISEs assayed here possess this motif, including the required double arginine thought to be an indicator of the NADPH-dependent activity of PRISEs (Supplemental Fig. S5C) (Herl et al. 2009) and no other explanation could be hypothesized for PhCIRs NADH activity from the structural analysis. Moreover, Geu-Flores and coworkers also reported a PRISE with no cofactor preference, although having the GxxRR motif (Geu-Flores et al. 2012). Thus, more knowledge seems necessary to distinctively associate protein sequence and cofactor affinity. All enzymes, except PRISE-2 representative, were able to reduce progesterone but rather weakly (Supplemental Fig. S5B). Interestingly, PhCIR1a sequence appeared remarkably divergent compared with clade I sequences (43% of identity on average; Supplemental Fig. S5C). These results pointed out that the activity of pelargonium PRISEs toward a given substrate can vary but is not associated with the overall degree of sequence conservation.

Several phylogenies of PRISEs were previously built but were limited by the number of available sequences (Munkert et al. 2015; Nguyen and O'Connor 2020) or were obtained in a specific context (Tarrío et al. 2011). To better understand how PRISEs evolved in Chloroplastida and if PhCIRs could be related to a specific clade, public databases were searched in order to build a phylogeny of 754 protein sequences (Supplemental Fig. S6). Only a handful were retrieved in charophyte algae and were used to root the tree. Clades I, II, and III defined from the initial restricted set of sequences were identified and used to annotate the tree. All 3 clades appeared specific to angiosperms, with clade I possibly extending to gymnosperms, although only with low statistical support. The 3 clades could be essentially related to clades vi, iv, and v respectively as defined in Nguyen and O'Connor (2020). PRISEs from ferns constituted a sister group to extended clades I and II. This whole group appeared sister to the clade III and lycophyte sequences. Finally, bryophyte sequences were grouped in a monophyletic group, sister to all other PRISEs, to the exclusion of algae. Altogether, this phylogeny showed that PRISEs expanded greatly in land plants and mostly independently within each major group. Clade I underwent the largest expansion of all angiosperm clades.

To investigate how the clade II sequences evolved, PRISE phylogeny was mapped to a Chloroplastida tree, built from all the species found during sequence retrieval and presented at the level of the taxonomic order (Fig. 8). PRISEs were found in almost all land plant (Embryophyta) orders examined. Clade II was conserved in the majority of angiosperms spanned by the analysis, but not in the earliest divergent order of the Nymphaeales nor the Amborellales. Several orders are devoid of clade II sequences, albeit comprising numerous PRISEs (*e.g.* Rosales). This result indicated that clade II PRISEs

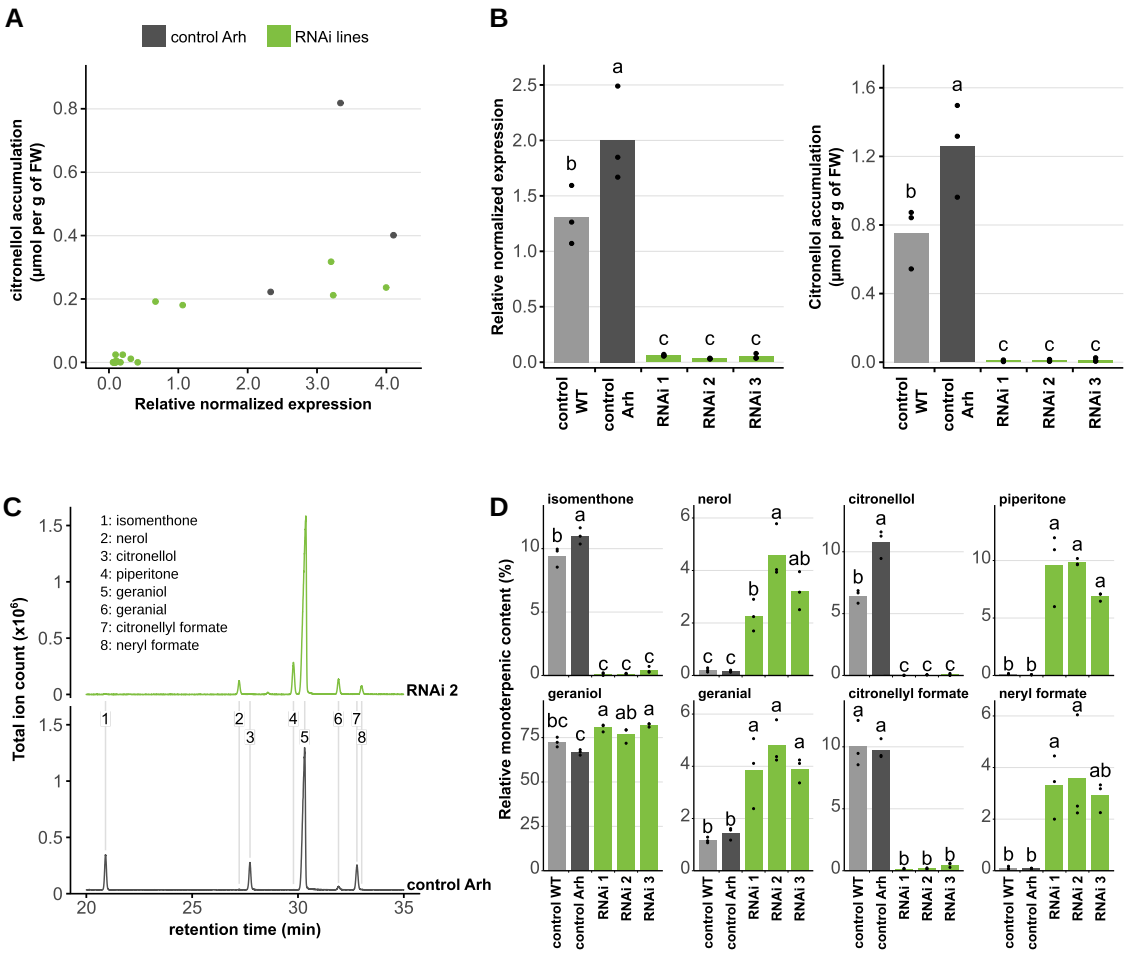

Figure 6. Accumulation of citronellol and other terpenes in PhCIRs RNAi plants. Transcript accumulation of *PhCIR1a*, *PhCIR1b*, and *PhCIR2* was altered in *A. rhizogenes*–mediated stable RNAi transformants of *P.* rosat 'Grasse' (RNAi lines). WT *P.* rosat 'Grasse' (control WT) and WT *A. rhizogenes* transformants (control Arh) were used as controls. Accumulation of citronellol and other compounds was assessed using GC-MS **A)** to **D)** and *PhCIRs* expression by RT-qPCR **A)** and **B)**; transcript accumulation was normalized to the geometric mean expression of *β-ACTIN* and *TCTP*. **A)** Citronellol content in function of PhCIR transcript accumulation of 18 independent transgenic RNAi lines and 3 WT *A. rhizogenes* transformants. **B)** Citronellol content and PhCIR transcript accumulation of 3 independent RNAi lines compared with wild-type (control WT) and transformation control lines (control Arh). **C)** Chromatogram of terpenes accumulated in a representative RNAi mutant (RNAi 2) compared with the transformation control. **D)** Detailed relative monoterpenic content of the 3 independent RNAi lines compared with the WT and transformation controls. **B)** and **D)** Barplots represent the mean ($n = 3$) and individual values are indicated with dots. Statistical differences between the different lines for each compound are outlined as letters per groups (ANOVA, followed by Tukey's test, $P < 0.05$).

likely evolved early during angiosperm history but had a complex evolutionary trajectory with losses in various orders.

Discussion

Citronellol biosynthesis in pelargonium depends on a multistep pathway starting from geraniol

In pelargonium, 3 hypothetical biosynthetic routes leading to the production of citronellol have been proposed. In this work, RNA sequencing (RNA-Seq), trichome-specific gene expression, in vitro and in planta enzymatic activities, as well as RNAi experiments unambiguously support that, as in *C. plicata* (Xu et al. 2017), pelargonium synthesizes citronellol in a multistep manner, involving several closely related PRISEs that act on citral. It is of note that pelargonium OPRs have the capacity to reduce citral in vitro (Iijima et al. 2016) and that NUDIX participation in citronellol formation might explain the accumulation of CP in pelargonium leaves (Bergman et al. 2021). However, the complete lack of detectable citronellol in transgenic plants that did not accumulate *PhCIR* transcripts shows that the contribution of other pathways in pelargonium must be at most minor. We note that since we did not check that the other pelargonium PRISEs were not silenced in the RNAi transformants, their participation to citral reduction cannot entirely be ruled out. If that were to be the case, these other PRISEs would likely produce minute amount of citronellal given their level of expression, by 1 or 2 orders of magnitude less as compared with PhCIRs.

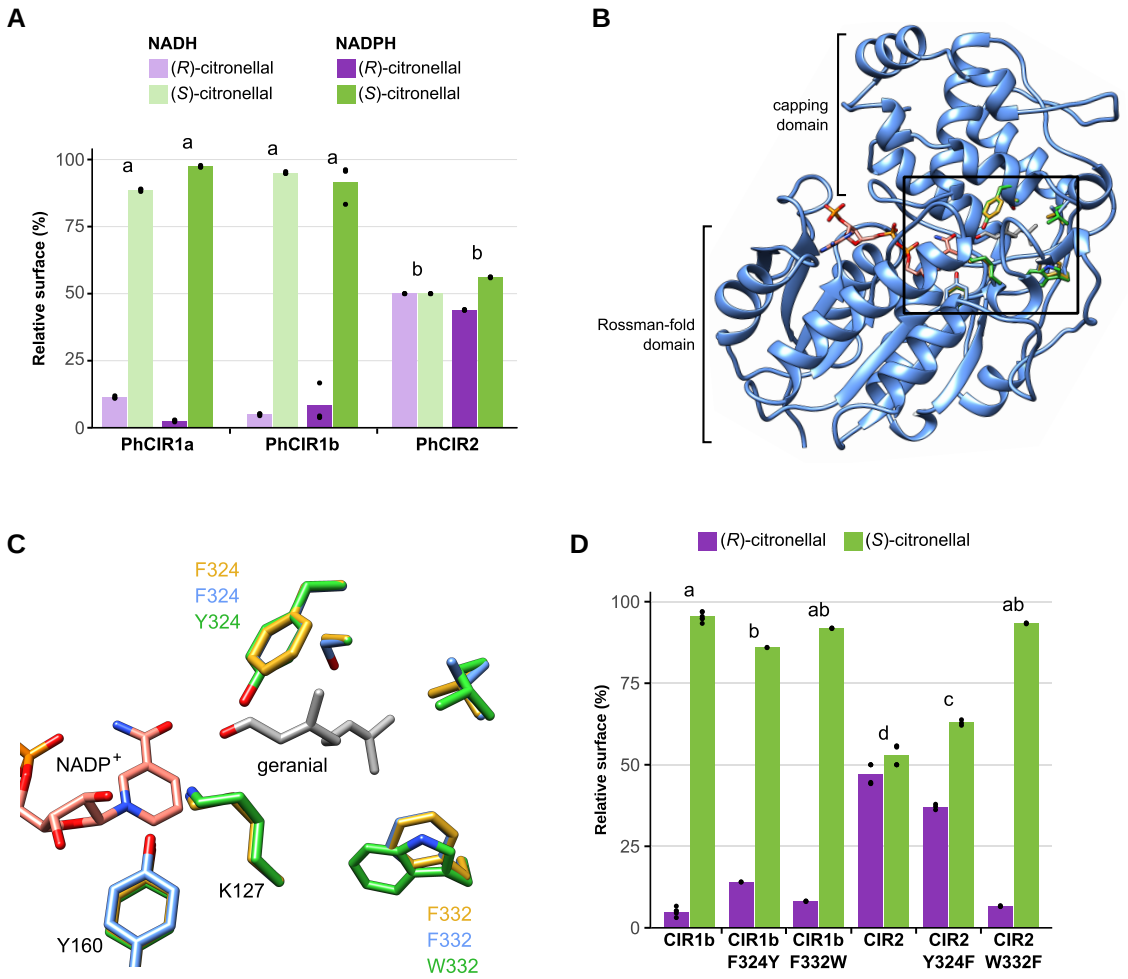

Figure 7. Enantioselectivity of PhCIRs explained by protein modeling and site-directed mutagenesis. **A)** Enantiomeric distribution of citronellal produced by the 3 PhCIRs assessed by chiral GC-FID analysis of extracts from in vitro enzymatic assays in the presence of citral and reduced cofactors. **B)** Overall structural model of the 3 superimposed PhCIRs. Both Rossman-fold domain and capping domain, characteristic of the PRISE family, are indicated. **C)** Close-up (black-box in **B)**) of the active site structure and structural representation of the amino acid variations. **B)** and **C)** Homology modeling of the proteins (yellow, PhCIR1a; blue, PhCIR1b; green, PhCIR2) was obtained with MODELLER using PmMOR from *P. major* (Fellows et al. 2018) as protein template (PDB identifier 5MLR). The positions of the geranial substrate and $NADP^+$ cofactor obtained from the PmMOR crystal structure were kept in order to compare structural features of the enzyme active sites. Atom colors as follows: red, oxygen, and blue, nitrogen. **D)** Enantiomeric distribution of citronellal produced by PhCIR1b, PhCIR2, and their respective mutants assessed by chiral GC-FID analysis of extracts from in vitro enzymatic assays in the presence of citral and NADH. **A)** and **D)** Barplots represent the mean percentage ($n = 3$) of each enantiomer, and individual values are depicted with dots. Statistical differences between enantiomeric ratios are outlined as letters per groups (ANOVA, followed by Tukey's test, $P < 0.01$).

That PhCIR enzymes reduced citral to citronellal, but not geraniol, is in line with the known mechanism of PRISEs, which requires an activated C=C double bond (Durchschein et al. 2012; Schmidt et al. 2018). These double bonds are only found next to a carbonyl, thus forming an enone group; this implies the participation of other oxidoreductases to convert geraniol to geranial and citronellal to citronellol. ADHs of the medium-chain dehydrogenase/reductase (MDR) superfamily, which have been characterized in sweet basil and perilla plants, are known to be able to catalyze the oxidation of geraniol to citral, as well as the reverse reduction of citral to geraniol and nerol (Iijima et al. 2006; Sato-Masumoto and Ito 2014). Moreover, an MDR-ADH is involved in the *C. plicata* pathway to oxidize geraniol to geranial and reduce citronellal to citronellol (Xu et al. 2017). In our study, it is likely that pelargonium trichomes express 1 or several ADHs acting on geraniol and citronellal. Equilibrium between these different catalytic reactions raises interesting questions as to the abundance of substrates, intermediates, and end products of the pathway. It could also explain why citronellal is barely observed in the 10 accessions, except in *P.* × 'Toussaint', or how citral can be accumulated to the detriment of geraniol in *P. citronellum*. Characterization of ADHs in pelargonium will provide answers to these questions and is actively under way.

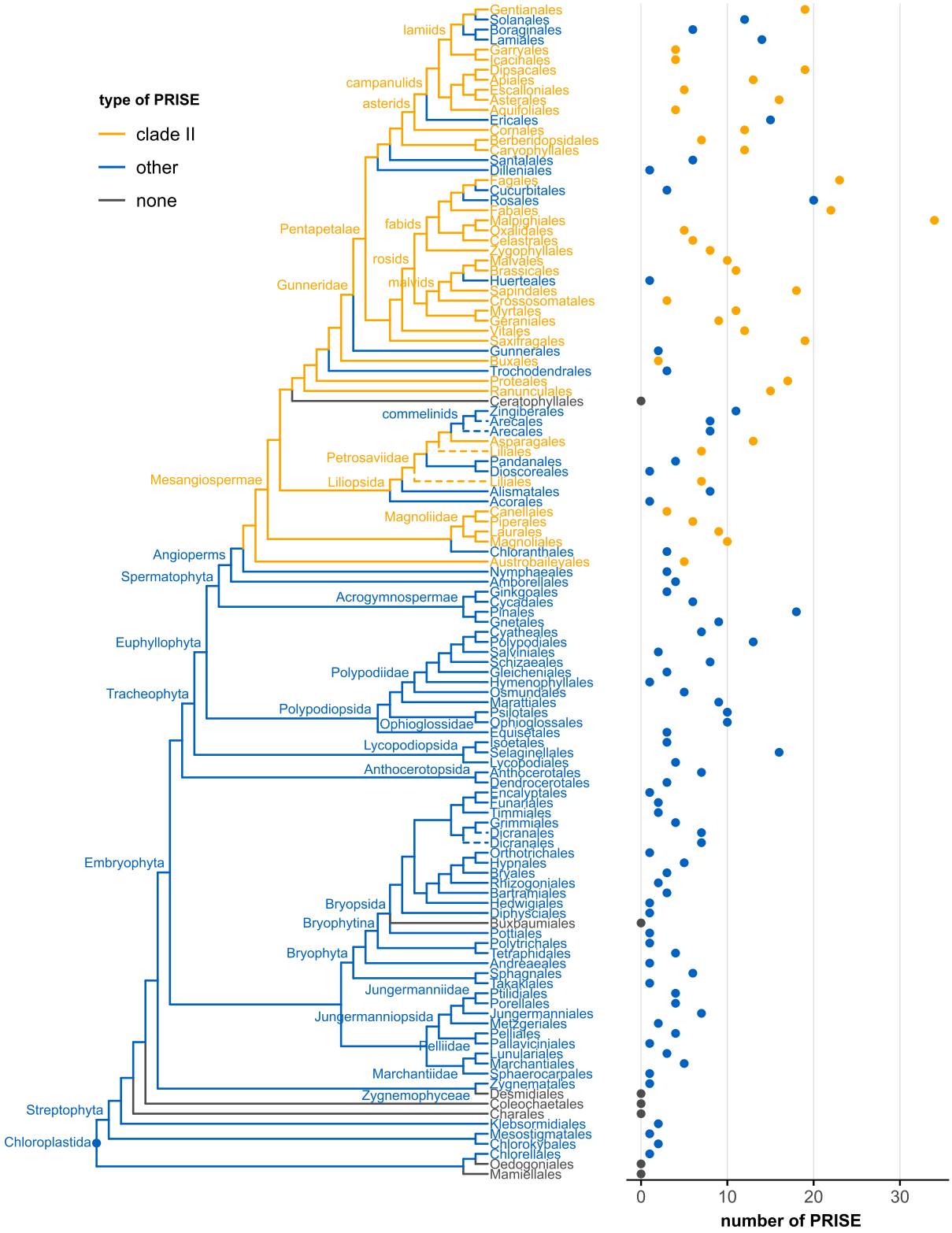

Figure 8. Evolution of PhCIR phylogenetic clade. Taxonomic orders associated with PRISE sequences retrieved in Chloroplastida (see Supplemental Fig. S6 and Data Set 2) were manually obtained from the National Center for Biotechnology Information (NCBI) taxonomy database using species name. Orders were used to induce a tree using the Tree of Life Web Project (tolweb.org). Because some taxonomic orders were not resolved as monophyletic, species names were used instead leading to paraphyletic or polyphyletic groups. When paraphyletic groups were located at the tip of a branch, monophyletic representation was obtained by collapsing the group. Other cases are represented by a dash line. The total number of PRISEs found per taxonomic order is depicted.

The enantioselective production of citronellol depends on closely related PRISEs

Because of their chiral center, citronellal and citronellol exist as (*R*)- or (*S*)-enantiomers. Since citronellol is synthesized through citronellal, absolute configuration is determined by PhCIRs at the citral reduction step. Stereoselective activity has been repeatedly observed among PRISE members (Gärtner et al. 1994; Herl et al. 2006; Durchschein et al. 2012). The acronym P5βR itself derives from their ability to stereospecifically reduce progesterone to 5β-pregnane-3,20-dione but not to 5α-pregnane-3,20-dione. Similarly, the ability of PRISEs to stereospecifically reduce 8-oxogeranial has led to a distinction between ISY and epi-ISY enzymes, involved in the biosynthesis of either (*cis-trans*)-iridoids or (*cis-cis*)-iridoids, respectively (Kries et al. 2017). The mechanism controlling PRISEs' stereoselectivity has been studied extensively and depends on the protonation face of the substrate during the hydride transfer from the cofactor (Gavidia et al. 2007; Thorn et al. 2008; Kries et al. 2016, 2017). In the *C. roseus* (*cis-trans*)-iridoid synthase CrISY, when the substrate is citral, the hydride transfer is selective of the pro-(*S*) face and results in the production of (*S*)-citronellal exclusively (Kries et al. 2016, 2017). It is reasonable to assume that a similar mechanism is responsible for the main production of (*S*)-citronellal in PhCIR1a/b, whereas in PhCIR2, this pro-(*S*) face selectivity is altered. However, it seems rather difficult to draw a general scheme of which positions in the active site are of importance for the stereoselectivity of PRISEs. For example, in an attempt to convert CrISY in an (*R*)-selective enzyme, like the (*cis-cis*)-iridoid synthase AmISY from *Antirrhinum majus*, site-directed mutagenesis highlighted that, unlike for the pelargonium CIRs, the residue corresponding to the W332 of PhCIR1b (CrISY L352) had barely any effect on the enzyme stereoselectivity (Kries et al. 2017). In contrast, mutation of the residues corresponding to the F324 and S325 of PhCIR1b increased the production of (*R*)-citronellal from trace amounts to 17%. Thus, stereoselectivity of PRISEs is rather a consequence of the whole active site conformation, likely leading to small displacements of the substrate that alter the stereoselectivity of the catalytic reaction. This observation is confirmed by the fact that PhCIR2^{W332F} mutant and PhCIR1b had identical stereoselectivities, while PhCIR1b^{F332W} and PhCIR2 had not. In this regard, the exceptional sequence proximity between PhCIR1b and PhCIR2 outside the active site (Fig. 4A) provides an excellent opportunity to study precisely how and which amino acid and conformational changes might affect PRISE stereoselective mechanism.

Is evolution of pelargonium CIRs driven by a dual biosynthetic role?

Aside from their central role in citronellol biosynthesis, PhCIRs are likely involved in the *p*-menthane pathway, as suggested by the lack of accumulation of isomenthone in PhCIR RNAi plants and by the accumulation of PhCIR1a/b transcript in *P. graveolens* and *P. radens*, 2 mint-scented accessions. Even though isomenthone could be a downstream product of a citronellol-starting hypothetical pathway—although it has never been documented to occur in planta (Chuah et al. 2001; Jacob et al. 2003)—accumulation of piperitone in RNAi plants points more to an active role of PhCIRs in the *p*-menthane pathways. An attractive possibility would be that, in pelargonium, the C=C double bond reduction leading to isomenthone does not occur on isopiperitenone but rather on piperitone, as suggested by Bergman and colleagues (Bergman et al. 2020; Bergman and Phillips 2020). In vitro investigation of PhCIRs activities toward piperitone and other *p*-menthanes, as well as study of mint-scented pelargonium, will help clarify the situation.

PRISEs are well known for their substrate promiscuity, as they can reduce a vast array of substrates carrying an activated C=C double bond (Durchschein et al. 2012; Petersen et al. 2016). PRISE promiscuity is thought to be an ancestral trait responsible for the enzyme family's ability to be active in different metabolic pathways without evolutionary pressure toward efficiency for a specific substrate (Schmidt et al. 2018; Nguyen and O'Connor 2020). It has been suggested that PRISEs participate in primary metabolism reactions (Nguyen and O'Connor 2020) and that their involvement in iridoid and progesterone pathways may be accidental (Hult and Berglund 2007). It exemplifies that natural selection relies on available enzymes (Jacob 1977) and does not require all enzymes to fit perfectly into a specific pathway. This would account for PRISEs from noncardenolide species, such as At5β-StR (5β-steroid reductase) or PmMOR, having higher affinities toward progesterone than DlP5βR1, whose metabolic function is progesterone reduction in *Digitalis lanata* cardenolide biosynthesis (Herl et al. 2009; Fellows et al. 2018; Klein et al. 2021). This characteristic of PRISEs can certainly explain the reemergence of the ISY function in the genus *Nepeta* after its loss during *Nepetoideae* evolution (Lichman et al. 2020), as well as the evolution of citral reduction in pelargonium by PhCIRs. In the latter, it is of great interest to note that other PRISEs tested here (from clade I) were generally as efficient as PhCIRs in reducing citral. It seems that evolution favored, through strong transcriptional regulation, the use of PRISEs belonging to a phylogenetic clade (clade II) which has, as of yet, no clear biological role and whose enzymes have been lost numerous times during angiosperm evolution. It is of note that *C. plicata* citral reduction is ensured by an enzyme from another phylogenetic clade (clade I) and is more closely related to PRISEs involved in iridoid and cardenolide biosynthesis. For a functional and phylogenetic analysis of the family, see Nguyen and O'Connor (2020). It is an open question whether the selection and parallel evolution of PhCIRs could have been driven by the putative dual function of the enzymes. PhCIRs could be suited enough to act in both citronellol and *p*-menthane pathways, providing better evolutionary fitness by using the same enzyme for 2 biosynthetic routes. It also presents the possibility for the plant to fine-tune the diversity of terpenes

produced by regulating an enzyme located at the crossroads of 2 important biosynthetic pathways. In line with this possibility, Bergman and colleagues observed that pelargoniums containing high amounts of geraniol, citronellol, and other compounds of the pathway tended to accumulate low quantities of *p*-menthanes (Bergman et al. 2020). Conversely, pelargoniums with high amounts of *p*-menthanes accumulated little geraniol and derivatives. However, that such observations could simply be the consequence of a competition between the 2 pathways due to substrate availability or affinity cannot be excluded.

PhCIR2 transcripts seemed to accumulate to noticeable levels in rosat accessions only and are detected in *P. radens* (Fig. 3). This indicates that the enzyme might originate from this parent and raises a more general question about the role and evolution of PhCIR2 in pelargonium. This is particularly important since PhCIR2 is the enzyme that contributes the most to the formation of (*R*)-citronellol found in pelargonium EO (up to 50%, according to Ravid et al. (1992)). Because most of the accessions examined here are highly polyploid, assessing the exact relationships between such close transcripts is impossible. Thus, the 3 enzymes could be the product of allelic versions of the same locus, homologs deriving from species crossbreeding, or paralogous genes. Only genomic data and careful sequencing of the different accessions will provide answers to this question.

Materials and methods

Plant material

P. × *hybridum* cv. rosat and *Pelargonium* × 'Toussaint' were provided by IFF-LMR-Naturals from the respective location of culture. *P. capitatum*, *P. radens*, *P. citronellum*, and *Pelargonium* 'Prince of Orange' were supplied by Le Jardin Botanique de la tête d'Or, Lyon, and La Pépinière Heurtebise, Clansayes, while *P. graveolens* was supplied by INRAE, Angers. All plants were cultivated under a 16:8 h and 25:18 °C light:dark cycle.

RNA extraction, cloning procedures, and RT-qPCR analyses

For high throughput RNA-Seq and cloning, total RNA extraction was performed using a modified version from Chang et al. (1993) and Cock et al. (1997), as previously described in Blerot et al. (2018). cDNAs were obtained using the SuperScript III Reverse Transcriptase (Invitrogen, #18080044) and cloned for further use in the GATEWAY pENTR/D-TOPO vector (Invitrogen, #K2400-20). PhCIR mutants were obtained by 2-step PCR-based site-directed mutagenesis as described by Ho et al. (1989). PhCIR RNAi construct was produced thanks to a sense and an antisense copy of a 306 bp sequence targeting the transcripts and obtained by PCR before being cloned in the pK7GWIWGII(I) plasmid (Karimi et al. 2002). Heterologous expression was achieved by transferring the coding sequence either to the pHXGWA vector (Busso et al. 2005) for recombinant protein production or the pK7WG2D (Karimi et al. 2002) for *N. benthamiana* transformation. All Gateway LR reactions were carried out using the LR-Clonase II Enzyme Mix (Invitrogen, #11791-020). Cloned sequences were checked by Sanger sequencing (Eurofins Genomics), and sequence verification and alignment were performed using the Geneious software. For RT-qPCR analyses, RNA was extracted using the Spectrum Plant Total RNA Kit (Sigma, #STRN250-1KT) according to manufacturer's instructions. cDNAs were obtained using the All-In-One RT MasterMix (Euromedex, #AM-G592) and RT-qPCR was performed as described in Blerot et al. (2018). All primers used for PCR reactions are listed in Supplemental Table S2.

Enzymatic assays

Escherichia coli Rosetta (DE3) pLysS cells (Novagen, Germany) were transformed with the appropriate vector, and recombinant proteins were obtained as described in Blerot et al. (2018). Enzymatic assays were performed at least in triplicates, using a protocol adapted from Xu et al. (2017) with slight modifications: 10 μg of purified recombinant proteins were incubated for 45 min in a 100 μL reaction with 2 mM of cofactor and 1 mM of substrate. NADH (#N8129), NADPH (#N6130), citral (#W230316), (*S*)-citronellal (#373753), β-citronellol (#27483), geraniol (#41090050), and progesterone (#P0130) were purchased from Sigma.

N. benthamiana leaf disc assays

Plant expression vector and P19 viral silencing suppressor (Voinnet et al. 2003) were transformed into the *Agrobacterium tumefaciens* strain LBA4404 (Invitrogen, #18313-015). Agrobacteria cultures were then coinfiltrated in *N. benthamiana* leaves according to Karimi et al. (2002). After 4 d, leaf discs were excised from transformed leaves and incubated for 3 h on 10 mL phosphate citrate buffer (20 mM, pH7.4) containing 400 μM of substrate in Petri dishes according to Höfer et al. (2013). Leaf disc terpene content was then extracted with 2 mL hexane.

Subcellular localization of PhCIR1a

PhCIR1a coding sequences deprived of terminal codon stop were transferred into the pMDC83 in planta expression vector (Curtis and Grossniklaus 2003), to generate a fusion protein with GFP fused to the C-terminal part of the protein. To determine subcellular localization of the target protein, infiltrated leaf sectors of *N. benthamiana* were observed after 4 d using a TCS-SP2 inverted confocal scanning laser microscope (Leica Microsystems) with a ×40/0.80W lens. The argon laser was set at 488 nm for GFP excitation and the helium-neon laser at 633 nm for chlorophyll. The fluorescent signals were captured through narrow bands: 500 to 550 nm for GFP and 640 to 740 nm for chlorophyll. Primers used for cloning are listed in Supplemental Table S1. Leaves infiltrated only with agrobacteria transformed to express the gene encoding the P19 viral suppressor provided a negative control

of GFP fluorescence. In silico prediction of PhCIR1a subcellular localization was realized with the help of TargetP and SignalP (Emanuelsson et al. 2007).

Production of RNAi lines by *A. rhizogenes*–mediated transformation

PhCIR RNAi construct was introduced into *A. rhizogenes* strain 15834 (kindly provided by Jean-Louis Hilbert and Caroline Rambaud, INRA, Nancy, France) by electroporation as described by Nagel et al. (1990). The transformed agrobacteria were grown onto YEB (Vervliet et al. 1975) medium with spectinomycin (50 $mg.L^{-1}$) at 28 °C. A starter culture was prepared from an isolated colony and incubated overnight under the same conditions and 180 rpm. Fifty mL of YEB medium was inoculated with the starter culture and incubated until an OD_{600} of 0.5 to 0.8 was reached. Cells were harvested by centrifugation (4,500 × *g*, 8 min) and washed 3 times with YEB. Plant transformation and shoot regeneration were performed as described by Pellegrineschi and Davolio-Mariani (1996) with the following modifications: explants used for inoculation were petioles from sterile *P.* rosat 'Grasse' cut into 1 cm segments; hairy roots were subcultured every 3 wks on mass spectrometry (MS)/5 solid medium supplemented with kanamycin (100 $mg.L^{-1}$) and cefotaxim (200 $mg.L^{-1}$); after 6 wks, shoots were initiated by adding cytokinin and auxin to the culture medium as described by Singh et al. (2017). Plants were then kept on MS/2 medium with the same mix of antibiotics until new roots were differentiated. Once grown enough, plants were potted into compost (TS3 bedding substrate, Heliogreen, #272527) containing 25% (*v*/*v*) perlite. Sampling for gas chromatography (GC)-MS analyses and RT-qPCR was performed 2 months after acclimation.

GC analyses

Terpenes were extracted overnight at 4 °C in hexane supplemented with an internal standard, either methylundecanoate or camphor, for relative quantification. GC-MS analyses were performed on a Agilent GC 6850 coupled with Agilent 5973 mass detector as described in Blerot et al. (2018), except for the oven settings set as follows: 60 °C 1 min, 60 to 245 °C 3 $°C.min^{-1}$, and 245 °C 4 min. For RNAi experiments, oven was set as 60 °C 1 min, 60–115 °C 1 $°C.min^{-1}$, 115–320 °C 15 $°C.min^{-1}$, and 320 °C 3 min and a split ratio of 10:1 was used. Data were analyzed using MSD ChemStation Data Analysis software. Compound identification was obtained by comparing retention time, retention index (Van Den Dool and Kratz 1963; Kovats 1965), and standard mass spectra using a mass spectrum database (Adams 2017). Chiral GC-FID analyses of citronellal were performed on an Agilent GC-FID 6890N using a Supelco β-DEX 225 column. A volume of 1 μL was injected at 250 °C and 6.76 psi without split at a constant flow rate of 1 $mL.min^{-1}$ of H_2. Oven was set as follows: 65 °C 5 min, 65–105 °C 1 $°C.min^{-1}$, 105–180 °C 15 $°C.min^{-1}$, and 180 °C 10 min.

Transcriptomic analyses

RNA extracts with a RNA integrity number higher than 6.5 were sequenced by BGI Tech Solutions (Hong Kong, China), using 4 lanes in an Illumina HiSeq X Ten platform. About 40 to 50 million paired-end reads were obtained per sequencing reaction. The quality of the reads was checked using fastQC (Andrews 2010) and cleaned using SortMeRNA v2.1 (Kopylova et al. 2012), Trimmomatic v0.36 (Bolger et al. 2014), and a collection of custom Perl scripts (v5.26). Clean reads were corrected using SPAdes v3.10.1 (Bankevich et al. 2012), khmer v2.1.1 (Crusoe et al. 2015), and ErrorCorrectReads.pl script from ALLPATHS-LG pipeline (Gnerre et al. 2011). De novo transcriptome assembly was performed using a pipeline based on SGA assembler v0.10.15 (Simpson and Durbin 2010) as described in Bonnot et al. (2017). Contigs were deduplicated and rectified with CAP3 (2/10/15) (Huang and Madan 1999), SSPACE v3.0 (Boetzer et al. 2011), and Pilon (Walker et al. 2014). Coding sequences were predicted from transcripts using a pipeline based on InterProScan 5.24–63.0, BLAST v2.6.0 using UniProt database (uniprot.org), and TransDecoder v3.0.1 (github.com/TransDecoder/TransDecoder). Transcripts containing several putative ORFs were detected during this step and split. Contigs encoding PRISE and OPR sequences were manually refined in order to elongate and deduplicate transcripts with the help of vsearch v2.13.6 (Rognes et al. 2016). Transcript expression was calculated using RSEM v1.3.1 (Li and Dewey 2014) and is available in Supplemental Data Set 1. *P.* rosat 'Grasse' long reads were obtained from cDNA sequencing following manufacturer's protocol (SQK-DCS109, Oxford Nanopore) on a MinIon device using a FLO-MIN106 flow cell. Data were basecalled using guppy v5.0.11+2b6dbffa5 in high accuracy mode then length (>300) and quality filtered (>8) using NanoFilt v2.8.0 (De Coster et al. 2018). An in-house Perl script using a strategy of self-blasting and homology search with the short-read assembled transcriptome of *P.* rosat 'Grasse' was applied to remove duplicated part of the original mRNA molecule. Adapters were removed using Porechop v0.2.4 (github.com/rrwick/Porechop). Homopolymers at both ends and long spurious reads were removed using in-house Perl scripts. A final length and quality filtering was applied before assembly using flye v2.9-b1768 (github.com/fenderglass/Flye). Quantification was obtained by mapping the reads with minimap2 v2.22-r1101 (Li and Dewey 2014) and salmon v1.6.0 (Patro et al. 2017).

Phylogenetic and statistical analyses

Sequences were retrieved from the different databases (see appropriate figure legends as well as Supplemental Data Set 2) by homology search using BLAST v2.6.0 and a minimum evalue of 1.10^{-3}. Sequences were aligned with clustalΩ v1.2.4 (Sievers et al. 2011), and the resulting alignment was manually edited to remove nonhomologous sites and obvious misalignments. Remaining identical sequences were deduplicated before maximum-likelihood

phylogenetic trees were inferred using RAxML v8.2.11 (Stamatakis 2014) and an appropriate evolutionary model as determined with the help of ModelTest-NG (Darriba et al. 2019). Bootstrap values were computed during the RAxML run using the automatic bootstrap convergence criterion. We used *t* test and ANOVA to evaluate the role of the characterized PRISEs in the production of citronellol in pelargoniums. Tukey's test was the only post-hoc test performed, when multiple comparisons were required. To compare the enzymes efficiency with citral, a *t* test was performed for the cofactor affinity of each enzyme and 1-way ANOVAs followed by Tukey's tests were used to compare the activity of the 3 different PhCIRs, either with NADH or NADPH. Similarly, a 1-way ANOVA followed by a Tukey's test was performed to compare the enantiomeric distribution of all PhCIRs and their mutants. RT-qPCR results for PhCIRs expression in leaves with or without trichomes were analyzed using a *t* test. For the RNAi experiments, a 1-way ANOVA, followed by a multiple comparison using a Tukey's test, was performed for each expression and accumulation profiles. Statistical analyses were carried out using R v4.2.1 and v4.3.1 (R Core Team, R-project.org); packages rotl v3.0.12 and ggtree v3.4.1 were used to create the Chloroplastida phylogenetic tree, while packages stats v4.3.1 and rstatix v0.7.2 were used for *t*, ANOVA, and Tukey's tests.

Protein modeling

Homology modeling was carried out with MODELLER (Webb and Sali 2016). The structure of *P. major* multisubstrate oxidoreductase PmMOR^{V150M} mutant available in complex with geranial and NADP^{+} (PDB entry: 5MLR) was used as a protein template (Fellows et al. 2018). The template sequence was selected following a homology search using BLAST with the UniProt database (https://www.uniprot.org/blast) and PhCIR1a as bait. Sequences were aligned with clustalΩ algorithm (Sievers et al. 2011). The homology models of PhCIR isoforms with the lowest normalized DOPE score and no steric clash were selected. Manual docking of the substrates was performed by superimposition of the models and the template, using the positions from the PmMOR crystal structure. Molecular graphics and analyses were performed with UCSF Chimera (Pettersen et al. 2004). An alternative model was obtained using the AlphaFold prediction algorithm (Jumper et al. 2021; Varadi et al. 2022). The comparison between AlphaFold and MODELLER models showed an RMSD below 1 Å and no additional information.

Accession numbers

Sequence data from this article are openly available from the GenBank data libraries under accession numbers OP680520 (prise-1), OP680521 (prise-2), OP680522 (prise-3-1), OP680523 (prise-3-2), OP680524 (PhCIR1a), OP680525 (PhCIR1b), and OP680526 (PhCIR2). Pelargonium short-read and long-read sequences are openly available from the Sequence Read Archive (SRA) database under the BioProject PRJNA883637 and PRJNA883613, respectively. Transcriptome assemblies are openly available from the Transcriptome Shotgun Assembly (TSA) database under the following accession numbers: *P. capitatum*, GKBW00000000; *P. graveolens*, GKCF00000000; *P. radens*, GKCH00000000; *P. citronellum*, GKCE00000000; *P.* 'Prince of Orange', GKCG00000000; *P.* rosat 'Grasse' short-read assembly, GKCN00000000; *P.* rosat 'Grasse' long-read assembly, GKCI00000000; *P.* rosat 'China', GKCL00000000; *P.* rosat 'Bourbon', GKCJ00000000; *P.* rosat 'Egypt', GKCK00000000; and *P.* × 'Toussaint', GKCM00000000.

Acknowledgments

We thank Jean-Louis Hilbert and Caroline Rambaud for providing *A. rhizogenes* strains, Sabine Palle for confocal microscopy help, Jean-Louis Magnard for helpful discussions, and Jonathan Gershenzon for his critical reading of the manuscript.

Author contributions

L.M., C.B., A.B., F.G., C.C., S.F., H.C., F.S., Ben.B., F.J., and D.S.-M. performed the research; G.C., Ber.B., and S.B. supported the research; L.M., C.B., S.F., F.J., and D.S.-M. analyzed the data; L.M., C.B., F.J., and D.S.-M. designed the research and wrote the paper.

Supplemental data

The following materials are available in the online version of this article.

Supplemental Figure S1. Expression of groups of orthologous transcripts of the OPR family in pelargonium.

Supplemental Figure S2. Assembled transcripts corresponding to PRISE-4 sequences in long-read transcriptome data.

Supplemental Figure S3. PhCIR1a activity and subcellular localization in *N. benthamiana* leaves.

Supplemental Figure S4. Nucleotide sequence alignment (protein-coding sequences) of the 3 PhCIRs and 1 sequence from the PRISE-3 ortholog group.

Supplemental Figure S5. Characterization of additional pelargonium PRISEs.

Supplemental Figure S6. Maximum-likelihood tree of 754 PRISE sequences.

Supplemental Table S1. Relative monoterpenic content in 4-d-old *N. benthamiana* leaf discs incubated with different substrates.

Supplemental Table S2. Sequences of primers used with their corresponding targeted gene and utilization.

Supplemental Data Set 1. Transcriptome expression data.

Supplemental Data Set 2. Databases and accession numbers of sequences used in phylogenies.

Funding

This work was supported by the grant number DRARI-6-775 from the French Agence Nationale de la Recherche and IFF-LMR Naturals through the framework of the Plan de Relance : Préservation de L'Emploi R&D.

Conflict of interest statement. None declared.

Data availability

The data underlying this article are available in its online supplementary material and different public repositeries as listed in the Materials and Methods Accession numbers section.

References

Adams RP. Identification of essential oil components by gas chromatography/mass spectrometry, Ed. 4.1 2017 .

Andrews S. FastQC 2010.

Bankevich A, Nurk S, Antipov D, Gurevich AA, Dvorkin M, Kulikov AS, Lesin VM, Nikolenko SI, Pham S, Prjibelski AD, et al. SPAdes: a new genome assembly algorithm and its applications to single-cell sequencing. J Comput Biol. 2012:**19**(5):455–477. https://doi.org/10.1089/cmb.2012.0021

Banthorpe DV, Long DRS, Pink CR. Biosynthesis of geraniol and related monoterpenes in *Pelargonium graveolens*. Phytochemistry 1983:**22**(11):2459–2463. https://doi.org/10.1016/0031-9422(83)80140-X

Bergman ME, Bhardwaj M, Phillips MA. Cytosolic geraniol and citronellol biosynthesis require a nudix hydrolase in rose-scented geranium (*Pelargonium graveolens*). Plant J. 2021:**107**(2):493–510. https://doi.org/10.1111/tpj.15304

Bergman ME, Chávez Á, Ferrer A, Phillips MA, Napier R. Distinct metabolic pathways drive monoterpenoid biosynthesis in a natural population of *Pelargonium graveolens*. J Exp Bot. 2020:**71**(1):258–271. https://doi.org/10.1093/jxb/erz397

Bergman ME, Phillips MA. Structural diversity and biosynthesis of plant derived p-menthane monoterpenes. Phytochem Rev. 2020:**20**(2):433–459. https://doi.org/10.1007/s11101-020-09726-0

Blerot B, Baudino S, Prunier C, Demarne F, Toulemonde B, Caissard JC. Botany, agronomy and biotechnology of Pelargonium used for essential oil production. Phytochem Rev. 2016:**15**(5):935–960. https://doi.org/10.1007/s11101-015-9441-1

Blerot B, Martinelli L, Prunier C, Saint-Marcoux D, Legrand S, Bony A, Sarrabère L, Gros F, Boyer N, Caissard J-C, et al. Functional analysis of four terpene synthases in rose-scented Pelargonium cultivars (*Pelargonium* × *hybridum*) and evolution of scent in the Pelargonium genus. Front Plant Sci. 2018:**9**:1435. https://doi.org/10.3389/fpls.2018.01435

Boetzer M, Henkel CV, Jansen HJ, Butler D, Pirovano W. Scaffolding pre-assembled contigs using SSPACE. Bioinformatics. 2011:**27**(4):578–579. https://doi.org/10.1093/bioinformatics/btq683

Bolger AM, Lohse M, Usadel B. Trimmomatic: a flexible trimmer for Illumina sequence data. Bioinformatics. 2014:**30**(15):2114–2120. https://doi.org/10.1093/bioinformatics/btu170

Bonnot C, Proust H, Pinson B, Colbalchini FPL, Lesly-Veillard A, Breuninger H, Champion C, Hetherington AJ, Kelly S, Dolan L. Functional PTB phosphate transporters are present in streptophyte algae and early diverging land plants. New Phytol. 2017:**214**(3):1158–1171. https://doi.org/10.1111/nph.14431

Burda E, Kraußer M, Fischer G, Hummel W, Müller-Uri F, Kreis W, Gröger H. Recombinant Δ4,5-steroid 5 β-reductases as biocatalysts for the reduction of activated C=C-double bonds in monocyclic and acyclic molecules. Adv Synth Catal. 2009:**351**(17):2787–2790. https://doi.org/10.1002/adsc.200900024

Busso D, Delagoutte-Busso B, Moras D. Construction of a set Gateway-based destination vectors for high-throughput cloning and expression screening in *Escherichia coli*. Anal Biochem. 2005:**343**(2):313–321. https://doi.org/10.1016/j.ab.2005.05.015

Chang S, Puryear J, Cairney J. A simple and efficient method for isolating RNA from pine trees. Plant Mol Biol Report. 1993:**11**(2):113–116. https://doi.org/10.1007/BF02670468

Chuah GK, Liu SH, Jaenicke S, Harrison LJ. Cyclisation of citronellal to isopulegol catalysed by hydrous zirconia and other solid acids. J Catal. 2001:**200**(2):352–359. https://doi.org/10.1006/jcat.2001.3208

Cock JM, Swarup R, Dumas C. Natural antisense transcripts of the S locus receptor kinase gene and related sequences in *Brassica oleracea*. Mol Gen Genet. 1997:**255**(5):514–524. https://doi.org/10.1007/s004380050524

Crusoe MR, Alameldin HF, Awad S, Boucher E, Caldwell A, Cartwright R, Charbonneau A, Constantinides B, Edvenson G, Fay S, et al. The khmer software package: enabling efficient nucleotide sequence analysis. F1000Research. 2015:**4**:900. https://doi.org/10.12688/f1000research.6924.1

Curtis MD, Grossniklaus U. A Gateway cloning vector set for high-throughput functional analysis of genes in planta. Plant Physiol. 2003:**133**(2):462–469. https://doi.org/10.1104/pp.103.027979

Darriba D, Posada D, Kozlov AM, Stamatakis A, Morel B, Flouri T. ModelTest-NG: a new and scalable tool for the selection of DNA and protein evolutionary models. Mol Biol Evol. 2019:**37**(1):291–294. https://doi.org/10.1093/molbev/msz189

De Coster W, D'Hert S, Schultz DT, Cruts M, Van Broeckhoven C. NanoPack: visualizing and processing long-read sequencing data. Bioinformatics. 2018:**34**(15):2666–2669. https://doi.org/10.1093/bioinformatics/bty149

Demarne F-E. 'Rose-scented geranium 'a Pelargonium grown for the perfume industry. In: **Lis-Balchin M**, editors. Geranium pelarg. London: Taylor & Francis; 2002. p. 205–223.

Demarne F-E, Van der Walt JJA. Composition of the essential oil of *Pelargonium citronellum* (Geraniaceae). J Essent Oil Res. 1993:**5**(3):233–238. https://doi.org/10.1080/10412905.1993.9698214

Doimo L, Mackay DC, Rintoul GB, D'Arcy BR, Fletcher RJ, D'Arcy BR, Doimo L, Rintoul GB, Fletcher RJ, Mackay DC, et al. Citronellol: geraniol ratios and temperature in geranium (Pelargonium hybrid). J Hortic Sci Biotechnol. 1999:**74**(4):528–530. https://doi.org/10.1080/14620316.1999.11511147

Dunphy PJ, Allcock C. Isolation and properties of a monoterpene reductase from rose petals. Phytochemistry 1972:**11**(6):1887–1891. https://doi.org/10.1016/S0031-9422(00)90148-1

Durchschein K, Wallner S, MacHeroux P, Schwab W, Winkler T, Kreis W, Faber K. Nicotinamide-dependent Ene reductases as alternative biocatalysts for the reduction of activated alkenes. Eur J Org Chem. 2012:**26**:4963–4968. https://doi.org/10.1002/ejoc.201200776

Duretto MF. Notes on Boronia (Rutaceae) in eastern and northern Australia. Muelleria. 2003:**17**:19–135. https://doi.org/10.5962/p.254918

Emanuelsson O, Brunak S, Von Heijne G, Nielsen H. Locating proteins in the cell using TargetP, SignalP and related tools. Nat Protoc. 2007:**2**(4):953–971. https://doi.org/10.1038/nprot.2007.131

Fellows R, Russo CM, Silva CS, Lee SG, Jez JM, Chisholm JD, Zubieta C, Nanao MH. A multisubstrate reductase from *Plantago major*: structure-function in the short chain reductase superfamily. Sci Rep. 2018:**8**(1):14796. https://doi.org/10.1038/s41598-018-32967-1

Gärtner DE, Keilholz W, Seitz HU. Purification, characterization and partial peptide microsequencing of progesterone 5β-reductase from shoot cultures of *Digitalis purpurea*. Eur J Biochem. 1994:**225**(3):1125–1132. https://doi.org/10.1111/j.1432-1033.1994.1125b.x

Gauvin A, Lecomte H, Smadja J. Comparative investigations of the essential oils of two scented geranium (Pelargonium spp.) cultivars

grown on Reunion Island. Flavour Fragr J. 2004:**19**(5):455–460. https://doi.org/10.1002/ffj.1354

Gavidia I, Tarrío R, Rodríguez-Trelles F, Pérez-Bermúdez P, Ulrich Seitz H. Plant progesterone 5β-reductase is not homologous to the animal enzyme. Molecular evolutionary characterization of P5βR from *Digitalis purpurea*. Phytochemistry 2007:**68**(6):853–864. https://doi.org/10.1016/j.phytochem.2006.11.019

Geu-Flores F, Sherden NH, Glenn WS, O'connor SE, Courdavault V, Burlat V, Nims E, Wu C, Cui Y. An alternative route to cyclic terpenes by reductive cyclization in iridoid biosynthesis. Nature 2012:**492**(7427):138–142. https://doi.org/10.1038/nature11692

Gnerre S, MacCallum I, Przybylski D, Ribeiro FJ, Burton JN, Walker BJ, Sharpe T, Hall G, Shea TP, Sykes S, et al. High-quality draft assemblies of mammalian genomes from massively parallel sequence data. Proc Natl Acad Sci U S A. 2011:**108**(4):1513–1518. https://doi.org/10.1073/pnas.1017351108

Herl V, Fischer G, Müller-Uri F, Kreis W. Molecular cloning and heterologous expression of progesterone 5β-reductase from *Digitalis lanata* Ehrh. Phytochemistry 2006:**67**(3):225–231. https://doi.org/10.1016/j.phytochem.2005.11.013

Herl V, Fischer G, Reva VA, Stiebritz M, Muller YA, Müller-Uri F, Kreis W. The VEP1 gene (At4g24220) encodes a short-chain dehydrogenase/reductase with 3-oxo-Δ4,5-steroid 5β-reductase activity in *Arabidopsis thaliana* L. Biochimie 2009:**91**(4):517–525. https://doi.org/10.1016/j.biochi.2008.12.005

Ho SN, Hunt HD, Horton RM, Pullen JK, Pease LR. Site-directed mutagenesis by overlap extension using the polymerase chain reaction. Gene 1989:**77**(1):51–59. https://doi.org/10.1016/0378-1119(89)90358-2

Höfer R, Dong L, André F, Ginglinger J-F, Lugan R, Gavira C, Grec S, Lang G, Memelink J, Van Der Krol S, et al. Geraniol hydroxylase and hydroxygeraniol oxidase activities of the CYP76 family of cytochrome P450 enzymes and potential for engineering the early steps of the (seco)iridoid pathway. Metab Eng. 2013:**20**:221–232. https://doi.org/10.1016/j.ymben.2013.08.001

Huang X, Madan A. CAP3: a DNA sequence assembly program. Genome Res. 1999:**9**(9):868–877. https://doi.org/10.1101/gr.9.9.868

Hult K, Berglund P. Enzyme promiscuity: mechanism and applications. Trends Biotechnol. 2007:**25**(5):231–238. https://doi.org/10.1016/j.tibtech.2007.03.002

Iijima M, Kenmoku H, Takahashi H, Lee JB, Toyota M, Asakawa Y, Kurosaki F, Taura F. Characterization of 12-oxophytodienoic acid reductases from rose-scented geranium (*Pelargonium graveolens*). Nat Prod Commun. 2016:**11**:1775–1782. https://doi.org/10.1177/1934578x1601101201

Iijima Y, Koeduka T, Suzuki H, Kubota K. Biosynthesis of geranial, a potent aroma compound in ginger rhizome (*Zingiber officinale*): molecular cloning and characterization of geraniol dehydrogenase. Plant Biotechnol. 2014:**31**(5):525–534. https://doi.org/10.5511/plantbiotechnology.14.1020a

Iijima Y, Wang G, Fridman E, Pichersky E. Analysis of the enzymatic formation of citral in the glands of sweet basil. Arch Biochem Biophys. 2006:**448**(1–2):141–149. https://doi.org/10.1016/j.abb.2005.07.026

Jacob F. Evolution and tinkering. Science 1977:**196**(4295):1161–1166. https://doi.org/10.1126/science.860134

Jacob RG, Perin G, Loi LN, Pinno CS, Lenardão EJ. Green synthesis of (−)-isopulegol from (+)-citronellal: application to essential oil of citronella. Tetrahedron Lett. 2003:**44**(18):3605–3608. https://doi.org/10.1016/S0040-4039(03)00714-7

Juliani HR, Koroch A, Simon JE, Hitimana N, Daka A, Ranarivelo L, Langenhoven P. Quality of geranium oils (Pelargonium species): case studies in southern and Eastern Africa. J Essent Oil Res. 2006:**18**(sup1):116–121. https://doi.org/10.1080/10412905.2006.12067131

Jumper J, Evans R, Pritzel A, Green T, Figurnov M, Ronneberger O, Tunyasuvunakool K, Bates R, Žídek A, Potapenko A, et al. Highly accurate protein structure prediction with AlphaFold. Nature 2021:**596**(7873):583–589. https://doi.org/10.1038/s41586-021-03819-2

Karimi M, Inzé D, Depicker A. GATEWAY™ vectors for Agrobacterium-mediated plant transformation. Trends Plant Sci. 2002:**7**(5):193–195. https://doi.org/10.1016/S1360-1385(02)02251-3

Klein J, Horn E, Ernst M, Leykauf T, Leupold T, Dorfner M, Wolf L, Ignatova A, Kreis W, Munkert J. RNAi-mediated gene knockdown of progesterone 5β-reductases in *Digitalis lanata* reduces 5β-cardenolide content. Plant Cell Rep. 2021:**40**(9):1631–1646. https://doi.org/10.1007/s00299-021-02707-3

Kopylova E, Noé L, Touzet H. SortMeRNA: fast and accurate filtering of ribosomal RNAs in metatranscriptomic data. Bioinformatics. 2012:**28**(24):3211–3217. https://doi.org/10.1093/bioinformatics/bts611

Kovats E. Gas chromatographic characterization of organic substances in the retention index system. Adv Chromotogr. 1965:**1**:229–247.

Kries H, Caputi L, Stevenson CEMM, Kamileen MO, Sherden NH, Geu-Flores F, Lawson DM, O'Connor SE. Structural determinants of reductive terpene cyclization in iridoid biosynthesis. Nat Chem Biol. 2016:**12**(1):6–8. https://doi.org/10.1038/nchembio.1955

Kries H, Kellner F, Kamileen MO, O'Connor SE. Inverted stereocontrol of iridoid synthase in snapdragon. J Biol Chem. 2017:**292**(35):14659–14667. https://doi.org/10.1074/jbc.M117.800979

Lalli JYY, Viljoen AM, Başer KHC, Demirci B, Özek T. The essential oil composition and chemotaxonomical appraisal of South African pelargoniums (Geraniaceae). J Essent Oil Res. 2006:**18**(sup1):89–105. https://doi.org/10.1080/10412905.2006.12067128

Li B, Dewey CN. RSEM: accurate transcript quantification from RNA-seq data with or without a reference genome. BMC Bioinformatics. 2014:**12**:323. https://doi.org/10.1186/1471-2105-12-323

Lichman BR, Godden GT, Hamilton JP, Palmer L, Kamileen MO, Zhao D, Vaillancourt B, Wood JC, Sun M, Kinser TJ, et al. The evolutionary origins of the cat attractant nepetalactone in catnip. Sci Adv. 2020:**6**(20):eaba0721. https://doi.org/10.1126/sciadv.aba0721

Lis-Balchin M. Essential oil profiles and their possible use in hybridization of some common scented geraniums. J Essent Oil Res. 1991:**3**(2):99–105. https://doi.org/10.1080/10412905.1991.9697917

Luan F, Mosandl A, Münch A, Wüst M. Metabolism of geraniol in grape berry mesocarp of *Vitis vinifera* L. cv. Scheurebe: demonstration of stereoselective reduction, E/Z-isomerization, oxidation and glycosylation. Phytochemistry 2005:**66**(3):295–303. https://doi.org/10.1016/j.phytochem.2004.12.017

Magnard JL, Roccia A, Caissard JC, Vergne P, Sun P, Hecquet R, Dubois A, Oyant LHS, Jullien F, Nicolè F, et al. Biosynthesis of monoterpene scent compounds in roses. Science 2015:**349**(6243):81–83. https://doi.org/10.1126/science.aab0696

Munkert J, Bauer P, Burda E, Müller-Uri F, Kreis W. Progesterone 5β-reductase of *Erysimum crepidifolium*: CDNA cloning, expression in *Escherichia coli*, and reduction of enones with the recombinant protein. Phytochemistry 2011:**72**(14–15):1710–1717. https://doi.org/10.1016/j.phytochem.2011.06.007

Munkert J, Pollier J, Miettinen K, Van Moerkercke A, Payne R, Müller-Uri F, Burlat V, O'Connor SE, Memelink J, Kreis W, et al. Iridoid synthase activity is common among the plant progesterone 5β-reductase family. Mol Plant. 2015:**8**(1):136–152. https://doi.org/10.1016/j.molp.2014.11.005

Nagel R, Elliott A, Masel A, Birch RG, Manners JM. Electroporation of binary Ti plasmid vector into *Agrobacterium tumefaciens* and *Agrobacterium rhizogenes*. FEMS Microbiol Lett. 1990:**67**(3):325–328. https://doi.org/10.1111/j.1574-6968.1990.tb04041.x

Nguyen T-DD, O'Connor SE. The progesterone 5β-reductase/iridoid synthase family is a catalytic reservoir for specialized metabolism across land plants. ACS Chem Biol. 2020:**15**(7):1780–1787. https://doi.org/10.1021/acschembio.0c00220

Patro R, Duggal G, Love MI, Irizarry RA, Kingsford C. Salmon provides fast and bias-aware quantification of transcript expression.

Nat Methods. 2017:**14**(4):417–419. https://doi.org/10.1038/nmeth.4197

Pellegrineschi A, Davolio-Mariani O. *Agrobacterium rhizogenes*-mediated transformation of scented geranium. Plant Cell Tissue Organ Cult. 1996:**47**(1):79–86. https://doi.org/10.1007/BF02318969

Pérez-Bermúdez P, Moya García AA, Tuñón I, Gavidia I. *Digitalis purpurea* P5βR2, encoding steroid 5β-reductase, is a novel defense-related gene involved in cardenolide biosynthesis. New Phytol. 2010:**185**(3):687–700. https://doi.org/10.1111/j.1469-8137.2009.03080.x

Petersen J, Lanig H, Munkert J, Bauer P, Müller-Uri F, Kreis W. Progesterone 5β-reductases/iridoid synthases (PRISE): gatekeeper role of highly conserved phenylalanines in substrate preference and trapping is supported by molecular dynamics simulations. J Biomol Struct Dyn. 2016:**34**(8):1667–1680. https://doi.org/10.1080/07391102.2015.1088797

Pettersen EF, Goddard TD, Huang CC, Couch GS, Greenblatt DM, Meng EC, Ferrin TE. UCSF Chimera—a visualization system for exploratory research and analysis. J Comput Chem. 2004:**25**(13):1605–1612. https://doi.org/10.1002/jcc.20084

Ravid U, Putievsky E, Katzir I, Ikan R, Weinstein V. Determination of the enantiomeric composition of citronellol in essential oils by chiral GC analysis on a modified γ-cyclodextrin phase. Flavour Fragr J. 1992:**7**(4):235–238. https://doi.org/10.1002/ffj.2730070413

Rognes T, Flouri T, Nichols B, Quince C, Mahé F. VSEARCH: a versatile open source tool for metagenomics. PeerJ. 2016:**4**:e2584. https://doi.org/10.7717/peerj.2584

Sato-Masumoto N, Ito M. Two types of alcohol dehydrogenase from Perilla can form citral and perillaldehyde. Phytochemistry 2014:**104**:12–20. https://doi.org/10.1016/j.phytochem.2014.04.019

Schmidt K, Petersen J, Munkert J, Egerer-Sieber C, Hornig M, Muller YA, Kreis W. PRISEs (progesterone 5β-reductase and/or iridoid synthase-like 1,4-enone reductases): catalytic and substrate promiscuity allows for realization of multiple pathways in plant metabolism. Phytochemistry 2018:**156**:9–19. https://doi.org/10.1016/j.phytochem.2018.08.012

Sievers F, Wilm A, Dineen D, Gibson TJ, Karplus K, Li W, Lopez R, McWilliam H, Remmert M, Söding J, et al. Fast, scalable generation of high-quality protein multiple sequence alignments using Clustal Omega. Mol Syst Biol. 2011:**7**(1):539. https://doi.org/10.1038/msb.2011.75

Simpson JT, Durbin R. Efficient construction of an assembly string graph using the FM-index. Bioinformatics. 2010:**26**(12):i367–i373. https://doi.org/10.1093/bioinformatics/btq217

Singh P, Khan S, Kumar S, ur Rahman L. Establishment of an efficient Agrobacterium-mediated genetic transformation system in *Pelargonium graveolens*: an important aromatic plant. Plant Cell Tissue Organ Cult. 2017:**129**(1):35–44. https://doi.org/10.1007/s11240-016-1153-8

Stamatakis A. RAxML version 8: a tool for phylogenetic analysis and post-analysis of large phylogenies. Bioinformatics. 2014:**30**(9):1312–1313. https://doi.org/10.1093/bioinformatics/btu033

Suga T, Shishibori T. The biosynthesis of geraniol and citronellol in *Pelargonium roseum* Bourbon. Bull Chem Soc Jpn. 1973:**46**(11):3545–3548. https://doi.org/10.1246/bcsj.46.3545

Surburg H, Panten J. Common fragrance and flavor materials: preparation, properties and uses. 5th ed. Weinheim: John Wiley & Sons; 2006.

Tarrío R, Ayala FJ, Rodríguez-Trelles F. The VEin Patterning 1 (VEP1) gene family laterally spread through an ecological network. PLoS One 2011:**6**(7):e22279. https://doi.org/10.1371/journal.pone.0022279

Thorn A, Egerer-Sieber C, Jäger CM, Herl V, Müller-Uri F, Kreis W, Muller YA. The crystal structure of progesterone 5β-reductase from *Digitalis lanata* defines a novel class of short chain dehydrogenases/reductases. J Biol Chem. 2008:**283**(25):17260–17269. https://doi.org/10.1074/jbc.M706185200

Tian Q, Wang P, Xie C, Pang P, Zhang Y, Gao Y, Cao Z, Wu Y, Li W, Zhu MX, et al. Identification of an arthropod molecular target for plant-derived natural repellents. Proc Natl Acad Sci U S A. 2022:**119**(18):e2118152119. https://doi.org/10.1073/pnas.2118152119

Van Den Dool H, Kratz PD. A generalization of the retention index system including linear temperature programmed gas-liquid partition chromatography. J Chromatogr. 1963:**11**:463–471. https://doi.org/10.1016/S0021-9673(01)80947-X

Varadi M, Anyango S, Deshpande M, Nair S, Natassia C, Yordanova G, Yuan D, Stroe O, Wood G, Laydon A, et al. AlphaFold Protein Structure Database: massively expanding the structural coverage of protein-sequence space with high-accuracy models. Nucleic Acids Res. 2022:**50**(D1):D439–D444. https://doi.org/10.1093/nar/gkab1061

Verma RS, Chandra Padalia R, Chauhan A. Essential oils in food preservation, flavor and safety. Earth: Elsevier Inc.; 2016697704.

Verma RS, Rahman L, Verma RK, Chauhan A, Singh A. Post harvest storage method for rose-scented Geranium (*Pelargonium graveolens* L' Herit. ex Ait. J Essent Oil Bear Plants. 2013:**16**(5):693–698. https://doi.org/10.1080/0972060X.2013.862930

Vervliet G, Holsters M, Teuchy H, Van Montagu M, Schell J. Characterization of different plaque-forming and defective temperate phages in Agrobacterium strains. J Gen Virol. 1975:**26**(1):33–48. https://doi.org/10.1099/0022-1317-26-1-33

Voinnet O, Rivas S, Mestre P, Baulcombe D. An enhanced transient expression system in plants based on suppresion of gene silencing by the p19 protein of tomato bushy stunt virus. Plant J. 2003:**33**(5):949–956. https://doi.org/10.1046/j.1365-313X.2003.01676.x

Walker BJ, Abeel T, Shea T, Priest M, Abouelliel A, Sakthikumar S, Cuomo CA, Zeng Q, Wortman J, Young SK, et al. Pilon: an integrated tool for comprehensive microbial variant detection and genome assembly improvement. PLoS One 2014:**9**(11):e112963. https://doi.org/10.1371/journal.pone.0112963

Webb B, Sali A. Comparative protein structure modeling using MODELLER. Curr Protoc Bioinforma. 2016:**54**(1):5.6.1–5.6.37. https://doi.org/10.1002/cpbi.3

Xiang B, Li X, Wang Y, Tian X, Yang Z, Ma L, Liu X, Wang Y. Cloning and characterization of two iridoid synthase homologs from *swertia mussotii*. Molecules. 2017:**22**:1–14. https://doi.org/10.3390/molecules22081387

Xu H, Bohman B, Wong DCJ, Rodriguez-Delgado C, Scaffidi A, Flematti GR, Phillips RD, Pichersky E, Peakall R, Bohman B, et al. Complex sexual deception in an orchid is achieved by co-opting two independent biosynthetic pathways for pollinator attraction. Curr Biol. 2017:**27**(13):1867–1877.e5. https://doi.org/10.1016/j.cub.2017.05.065

Yuan T-T, Chen Q-Q, Zhao P-J, Zeng Y, Liu X-Z, Lu S. Identification of enzymes responsible for the reduction of geraniol to citronellol. Nat Prod Bioprospecting. 2011:**1**(3):108–111. https://doi.org/10.1007/s13659-011-0032-6

Zhang GQ, Liu KW, Li Z, Lohaus R, Hsiao YY, Niu SC, Wang JY, Lin YC, Xu Q, Chen LJ, et al. The Apostasia genome and the evolution of orchids. Nature 2017:**549**(7672):379–383. https://doi.org/10.1038/nature23897